KfK 5165
März 1993

Multilayer Insulation in Cryoequipment - a Study of Reference Literature

S. Jacob
Institut für Technische Physik

Kernforschungszentrum Karlsruhe

KERNFORSCHUNGSZENTRUM KARLSRUHE

Institut für Technische Physik

KfK 5165

Multilayer insulation in cryoequipment - a study of reference literature

S. Jacob*

*Central-Cryogenic Facility Indian Institute of Science, Bangalore 560012, India

Kernforschungszentrum Karlsruhe GmbH, Karlsruhe

Als Manuskript gedruckt

Kernforschungszentrum Karlsruhe GmbH
Postfach 3640, 7500 Karlsruhe 1

ISSN 0303-4003

Abstract

The reasons of KfK/ITP starting investigations of superinsulation have been occasionally unsatisfactory qualities of insulation in some cryostats and helium transferlines manufactured by industry companies in former times.

Investigations so far performed within the TESSI test facility were limited to temperatures down to 80 K and the attention had been concentrated on the mat type superinsulation envisaged for large cryostats. This program has been finished successfully.

The intention is now, to convert the test facility with a view to extend the range of operating temperatures down to 4 K and to use for comprehensive investigations of thermal insulation in cryoequipment. I.e., in addition to the investigation and upgrading of (super)insulation techniques in cryostats, the modification of the test facility should allow also testing and upgrading of cryotransferline-models and of cryocomponents in cryostats and cryotransferlines generally.

Therefore studies with the following objectives have been performed:

- Literature study with concern to worldwide experience and datas in cryo multilayer insulation techniques and in connection with existing test facilities on the subject of "thermal insulation in cryoequipment".
- Intercomparison of measurement principles and techniques and their advantages and drawbacks.

Superisolation in Kryoapparaten - eine Literaturstudie

Zusammenfassung

Die Gründe zur Erstellung und zum Betrieb des Teststandes für Superisolationsuntersuchungen TESSI lagen in früheren tlw. unbefriedigenden Isolationsqualitäten in von Industriefirmen gebauten Kryostaten und He-Transferleitungen.

Bisherige Untersuchungen in TESSI waren begrenzt auf Temperaturen zwischen Raumtemperatur und 80 K und das Hauptaugenmerk lag auf der für Großkryostate vorgesehenen Superisolation in Mattenform. Dieses Programm wurde inzwischen erfolgreich beendet.

Die Absicht ist jetzt, den Teststand umzubauen, um den Betriebstemperaturbereich bis auf 4 K auszudehnen und ihn für umfassende Untersuchungen im Bereich der thermischen Isolation in Kryoapparaten nutzen zu können. Dies bedeutet, daß zusätzlich zur Untersuchung und Verbesserung von (Super)isolations-Techniken in Kryostaten die Änderung von TESSI Test und Verbesserung von Kryotransferleitungen sowie von Kryostat- und Kryotransferleitungs-Bauteilen zulassen soll.

Aus diesem Grunde wurden Studien mit folgenden Zielsetzungen durchgeführt:

- Literaturstudium betreffs weltweiter Erfahrungen und Daten auf dem Gebiet der Superisolationstechnik sowie mit Bezug auf die bestehenden Teststände für Untersuchungen zur thermischen Isolation in Kryoapparaten
- Vergleich der Meßprinzipien und Meßtechniken und deren Vor- und Nachteile.

CONTENTS

SECTION 1: INTRODUCTION

1.0 Multilayer insulation

Multilayer insulation (MLI) is the most efficient cryogenic insulation available currently. Because of the most effective thermal performance of evacuated multilayer insulation, it is often termed as 'superinsulation'.

Multilayer insulation consists of several layers of closely spaced, low emissivity radiation reflecting shields, which are placed in a perpendicular direction to the heat flow. Each shield reflects a large percentage of the radiation it receives from an adjacent warmer shield. Theoretically, 'n' number of independently floating shields between the cold and warm boundaries of a cryogenic container can reduce the radiation exchange by a factor $(n+1)$. Assuming the shields and the container walls have the same emissivity ε, the radiation heat transfer $Q_r \simeq (I_2-I_1) \cdot \varepsilon/2(n+1)$, where $I = \sigma AT^4$ corresponds to the black body radiation. However in practice, a large number of shields can not be kept truely floating and to minimize direct thermal contact either the radiation shields are crinkled or embossed or low thermal conductivity spacers are interposed between the shields. Typical excamples for radiation shields are aluminium foils or aluminized Mylar film. Similarly thermal spacers can be glassfiber paper, polyester netting etc.

1.1 Heat transfer through multilayer insulation

The heat transfer through multilayer insulation comprises of radiation exchange between the shields, solid conduction through the shields and the thermal spacers across their area of contacts and residual gas conduction in the interspaces of the insulation layers. But these modes are not independent and they have complex interactions. For example, changes in the interlayer gas pressure not only changes the residual gas conduction but also the radiation and solid conduction component of heat transfer, since gas pressure changes cause shift in the temperature profile of the insulation.

Not only the modes of heat transfer have complex interactions, they are also dependent on a variety of parameters such as number of layers, layer density, contact pressure and area, boundary temperatures, gas pressure within the insulation, emissivity of the shields, absorption and scattering coefficients of thermal spacers etc. Further, due to the highly anisotropic characteristics of the

radiation shields, there exists a coupling between longitudinal and lateral heat conduction in multilayer insulations.

The above aspects make a meaningful comparison of different types of MLI rather difficult and even for the same insulation, the thermal effectiveness can vary, depending on the several parameters already mentioned. Still there exists a need to compare the insulation effectiveness of different types of MLI and to optimize the insulation parameters for specific applications. As a performance index parameter, a Fourier law type conductivity coefficient called 'apparent' or 'effective' thermal conductivity coefficient (K_{eff}) is often used for this purpose. Since the thickness of the insulation is small compared to physical dimensions of cryogenic systems, the heat transfer in MLI can be approximated to one dimensional for heat flow normal to the surface. Then

$$K_{eff} = Q\delta/A\,(T_h - T_c) \qquad (1)$$

where Q is the heat flow through the insulation in the normal direction, δ is the insulation thickness, A is the area and T_h and T_c are the warm and cold boundaries. However it should be clearly understood that K_{eff} is not a material property in the usual sense of thermal conductivity but only a performance indicator, accepted for the past 30 years by the cryogenic laboratories and industry. This complexity arises due to the non-linear temperature profile in the multilayer insulation, dependent on the radiation-conduction contribution [1]. Therefore one is unable to appreciate the concern of Halaczek and Rafalowicz [2] that the integral method is more suited to estimate K_{eff} in MLI than the differential method. The more important aspect appears to be the accuracy in measuring the true heat flux through the insulation and identifying the parameters associated with the measurement such as, shield and spacer characteristics, layer density, number of layers, boundary temperatures, vacuum level etc.

Scurlock and Scaull [3] estimated the ideal K_{eff} of an MLI for typical parameters (T_h = 293 K, T_c = 77 K, ε = 0.02 and ($n+1/\delta$ = 30 layers/cm) to be 0.065 $\mu Wcm^{-1}K^{-1}$. However in actual practice, calorimetric experimental values of K_{eff} obtained for a large number of investigations range approximately from 0.2 to 1 $\mu Wcm^{-1}\,K^{-1}$. Degradation in the thermal quality is experienced as compared to calorimetric experiments, when MLI is applied over real cryogenic equipment [4].

SECTION 2: MEASUREMENT OF HEAT FLUX IN MLI

2.0 Measurement techniques

The methods used for the evaluation of the thermal effectiveness of multilayer insulations can be broadly classified into (a) unsteady state methods (b) steady state methods.

The unsteady state method, as the name indicates, does not require the establishment of thermal equilibrium in the sample. The thermal diffusivity of the insulation sample can be estimated from the cooling rate of the sample and this provides an indirect estimation of thermal conductivity [5]. However apart from the poor accuracy of measurement in the unsteady state methods, its principal advantage of providing a quick estimation is often lost in the case of multilayer insulations, due to the long time of evacuation needed before the sample can be cooled down.

There are 4 major types of steady state methods used in the estimation of heat flux/effective thermal conductivity of multilayer insulations:

(a) Boil-off calorimetry.
(b) Electrical input method.
(c) Heat meter technique.
(d) Temperature decay measurement.

2.1 Boil-off calorimetry

The most commonly used method in the estimation of the thermal performance of multilayer insulation is up to now boil-off calorimetry. When the insulation is applied over the test section of a calorimeter containing a cryogenic fluid, the heat transport across the insulation can be estimated from the evaporation rate of the cryogen at steady state conditions, provided secondary heat currents are eliminated.

The heat flux through the insulation is given by the expression

$$\dot{q} = \dot{m} L_V \qquad (2)$$

where $\dot{m}$ is the mass rate of the cryogen evaporation and L_V is the latent heat of vapourisation. In most of the calorimetric estimations, there is a small but definite background heat leak q_B, entering the test vessel other than from the insulation test surface area. In order to obtain the true heat-flux through the insulation, this

background heat flux has to be deducted from the estimated $\dot{q}$ value. q_B is usually estimated, when the warm boundary of the test module is kept at the cold boundary temperature. In many cases, the evaporation rate is measured by volumetric methods, then the mass rate is given by

$$\dot{m} = \dot{v}\,\rho_o \;\frac{T_o}{P_o}\,\frac{P}{T} \tag{3}$$

where
$\dot{v}$ = volumetric flow rate
ρ_o = gas density at NTP (273 K and 760 mm Hg)
T_o = 273 K
P_o = 760 mm Hg
P = vapour pressure in the test section of calorimeter
T = Gas temperature at the flow meter.

However to estimate heatflux with a good degree of accuracy, some additional factors have to be taken into consideration.

(a) Correction for unaccounted vapour fraction of evaporation

As the cryogen level decreases in the calorimeter due to evaporation, a part of the evaporated vapour instead of venting out from the calorimeter, occupies the volume space of the liquid evaporated. Consequently the entire quantity of evaporated vapour does not reach the flow measuring device. Therefore a correction factor $c = \rho_{liq}/\rho_{liq}\text{-}\rho_{gas}$, which accounts for the non-metered fration of evaporation, is incorporated into mass flow rate and equation (3) can be expressed as

$$\dot{m} = c \cdot \left[\dot{v}\,\rho_o \;\frac{T_o}{P_o}\,\frac{P}{T} \right] \tag{4}$$

The correction factor C for various cryogenic fluids are given below valid for 1 bar saturated vapour conditions [6].

Cryogen	Oxygen	Nitrogen	Hydrogen	Helium
C	1.003	1.006	1.019	1.152

Thus the correct factor C is more important when the calorimeter fluid is liquid helium.

(b) Effect of sensible heat increase of the vapour fraction.

In boil-off calorimetry, it is assumed that all the heat flux through the insulation results in the evaporation of the cryogenic fluid. A rather wrong indication of lower heat flux could be obtained if some of the heat flux is used only in raising the sensible heat of the vapour fraction present in the calorimeter. The magnitude of this error depends on the volume fraction of vapour in the cryostat and the thermal conductivity of the innerwall of the calorimeter. The errors can be kept below 0.1 percent, if care is taken in using a high conducting material such as copper for the innerwall of the test chamber and the cryostat is kept nearly full during the test [7].

(c) Barometric pressure change.

If the vapour pressure in the calorimeter is not maintained constant, it can cause errors in the measurement of heat flux through the insulation. Thus atmospheric pressure variations are to be taken into consideration in boil-off calorimetric investigations of MLI. As the pressure increases, the boiling point of the cryogen in the calorimeter rises, causing supercooling of the fluid. Part of the heat flux will be then utilised to heat the fluid to its new boiling point and during this period, the measurements record a lower boil-off rate as compared with the heat flux. Conversely, as the barometric pressure decreases, the bulk fluid temperature comes down by evaporative cooling. This results in a higher boil-off measurement in excess of that due to heat flux through the insulation. The corrections due to the change in the barometric pressure are discussed by De Hann [7], Kaganer [8] and Leung et. al [9].

For small changes in atmospheric pressure, the rate of change of mass flow rate is given by [9]

$$\frac{dm_t}{dt} = V \cdot \left(\frac{C_s}{V_L \, L_V} \right) \left(\partial T/\partial P \right)_{sat} \frac{dP}{dt} \qquad (5)$$

where V = Container volume

C_s = Liquid specific heat at saturation

V_L = Volume of Cryogen

L_V = Latent heat of vapourisation

$(\partial T/\partial P)_{sat}$ = Slope of the temperature-vapour pressure curves

dP/dt = Rate of change of atmospheric pressure

Kaganer [8] states that atmospheric pressure frequently changes at the rate of 1 mm Hg/hour. For this condition, he estimates that the evaporation rate of a liquid oxygen container with 2.4 % rated evaporation, can vary 10 % of this value. The conditions become more critical for calorimeters when the normal evaporation rate is rather small and when using a fluid with low heat of vapourisation.

Though the changes in the evaporation rate due to barometric pressure variations can be estimated as discussed above, in practice it is not easy to make corrections. This is because for a new steady state evaporation rate to reach after an incidence of barometric pressure change will take usually several hours and during this period further pressure changes may occur. Hence special pressure controllers are used [10,11] in the vapour outlet of the test chamber to maintain a steady vapour pressure in the chamber.

(d) Effects of stratifiction and superheating

Stratification results in a higher fluid surface temperature than the bulk. Since vapour pressure over the fluid will be determined by the surface temperature of the fluid, in boil-off calorimetry stratification can result in non-equivalent measurement of evaporation rate due to heat flux.

At times, cryogens stored in a vented container can become superheated in the lower regions, while the surface is at the saturation temperture. At some instant, the superheated liquid starts moving up and boiling vigourously, sometimes even producing a geyering effect. These effects tend to vary the uniform evaporation rate expected from the calorimeter.
In order to minimize these thermal effects, copper strips or wool could be placed inside the test and guard chambers.

(e) Effect of large background heat leak

When the background heat leak becomes of comparable value with that of the heat flux through the test sample, the measurement can become unreliable. Anchoring the liquid fill and vapour vent tubes and sensor leads to the guard chamber is essential to reduce the effect, apart from proper radiation baffles for the test chamber.

For liquid helium calorimeter, thermoacoustic oscillation can take place in the vapourline, causing a large background heat leak. Cotton plugs can be used to reduce the acoustic oscillation in ventlines [9].

2.2 Electrical input method

In this method, the electrical energy dissipated thermally by a electrical heater, uniformly covering the test sample, is measured in order to estimate the thermal conductivity of the sample [2,12,13]. In most cases, the sample is of circular profile. The main measurement heaters are guarded by compensating heaters and guard heaters, whose temperatures are controlled through feed-back circuits, so that the entire electrical energy input to the measurement heater will pass through the insulation sample. While the warm boundary temperature for measurement is provided by the measurement heater plate, the cold boundary temperature is obtained from the flat bottom plate of the cryogen tank.

2.3 Heat meter technique (pl. see section 4.5 also)

In the heat meter technique, one side of the test specimen has a constant temperature heat source and at the opposite side, a constant temperature heat sink is connected in series thermally through the heat meter [14,15]. Since under steady-state conditions, the same amount of heat flux passes through the test sample and heat meter (provided that there is no thermal exchange with the environment), estimation of the heat flux through the heat meter aids to find out the heat flux through the test sample. The heat meter is essentially a material of known thermal conductivity values over the temperature range of measurement, with provisions for two temperature sensors and a calibration heater, so that a thermal conductance measurement can be made. Knowing the temperature difference across the heat meter for different calibration heat loads, it will be possible to calibrate the apparatus and estimate the heat flux through the sample, placed in series with the heat meter and shielded from external heat sources.

2.4 Temperature decay measurement

This is essentially a non-cryogenic technique for quick evaluation of approximate thermal effectiveness of multilayer insulations. In this method, the temperature decay along an insulated tubular fin is measured [16] and the decay length 'L' is given by

$$L = | \lambda t / H_c |^{1/2} \quad (6)$$

where λ = average thermal conductivity of the tube
t = wall thickness
H_c = average heat transfer coefficient for MLI test sample.

The insulation to be tested is wrapped around a stainless steel tube of known wall thickness 't' and the insulated tube is placed inside a vacuum envelope, supported by low conducting supports. A heater attached to one side of the insulated tube, causes a heat flow along the tube. A steady state temperature profile along the insulated tube can be characterised by a decay length 'L', which results from the balance between longitudinal heat conduction along the tube wall and the transverse heat conduction through MLI.

SECTION 3: CALORIMETRIC MEASUREMENTS

3.0 Types of calorimeters

Different types of calorimeters are employed for measuring heat flux through multilayer insulation, either using the boil-off measurement method or the electrical input method. Depending on the method, the boundary temperatures for the measurement and the scope of the investigations in specific cases, each calorimeter can be expected to have unique features. However based on configuration aspects, calorimeters can be broadly classified into

(a) Cylindrical calorimeters
(b) Flate plate calorimeters
(c) Tank calorimeters

[Cryostats using heat leak meter method are discussed under section 4.5 and 5.4].

3.1 Cylindrical calorimeters

The first design of a cylindrical calorimeter was developed by Kropschot et al. [1] at the National Bureau of Standards, U.S.A. A schematic of the double guarded cylindrical calorimeter is shown in Fig. 1. The test chamber is shielded by bottom and top guard chambers, which contain the same cryogenic fluid as the test chamber but at a slightly higher vapour pressure ($\Delta P = 1 - 3$ Torr) in order to prevent recondensation of the evaporating vapours from the test chamber on its way to the flow meter through vapour ventline. The test sample of MLI is wrapped over the test and guard chambers.

Coston and Zierman [17] have optimized the lengths of the guard sections of the cylindrical calorimeter to reduce coupling of longitudinal conduction (which is 10^3 - 10^5 times larger than in the normal direction for MLI due to its highly anisotropic characteristics) with the heat flux in the normal direction. Thus the lengths of the guard sections of their cryostat are longer than the NBS design.

For calorimeters with cold boundary temperature below 77 K, additional guard chambers or cooling caps are needed [11,17].

3.2 Flat plate calorimeters

Flat plate calorimeters can be basically classified into two groups (a) guarded hot plate (b) guarded cold plate. In the guarded hot plate calorimeter, the heat flow through the insulation test specimen is assumed to be indentical to the heat supplied to the specimen from the hot boundary (either electrical or thermal heating) [12,13,18]. In the guarded cold plate version the heat removed from the insulation specimen serves as a measurement of the heat flow through the specimen, on the assumption that the heat removed is identical to the heat flow through the specimen (measured as the evaporation rate of the cryogen in the test chamber, in contact with the insulation). While for measurements at liquid nitrogen temperatures, single guarded cold plate is commonly used [19], for lower temperatures double guarded versions are used [10].

Flat plate calorimeters with guarded cold plate can be again of two versions (a) the plate in the horizontal plane [10,19] (b) the plate in the vertical orientation with respect to the cryogen vessel [9,20,21].

A typical double guarded cold-plate calorimeter is shown in Fig. 2. In the centre of the calorimeter is the measurement cryogen chamber (a), providing a part of the cold boundary surface to the insulation. The guard vessel (b) encapsulates the meausrement cryogen chamber (a), except at the cold boundary. Since both chambers have the same cryogen, the guard provides a nearly adiabatic surface around the measurement chamber. An outer guard vessel (f) is filled with LN_2, if the measurement chamber and the inner guard have LHe/LH_2 as the fluid. Another unique feature of flat plate calorimeters is that the effect of compression can be studied by applying uniform compressive load over the entire test area [22]. The warm boundary is provided by a regulated fluid heat exchanger or electrical heater assembly consisting of a measurement heater and a guard heater system.

3.3 Tank calorimeter

Tank calorimeters represent an insulation test system, closer to its actual application on a cryogenic container suspended from its neck tube. The insulation is applied over the entire surface of the calorimeter, unlike in the cases of cylindrical and flat plate calorimeters. Therefore, for insulation thermal tests in the temperature range of 300 - 77 K, there is no need for a guard chamber, except for reducing conduction down the neck tube. However for tests at lower

temperatures, guard chambers/radiation shields cooled down to 77 K are usually employed.

Fig. 3 shows a typical tank calorimeter. The tank is made of 0.25 inch thick copper and has torispherical heads. It is suspended by a 5 inch diameter stainless steel pipe. Cold guard and radiation baffles cooled by liquid nitrogen are fixed on to the top of the support tube. Since the calorimeter is designed for cold boundary at liquid hydrogen temperature, radiation shields enclosing the test chamber are provided.

The heat flux estimation in a tank calorimeter test of MLI is usually obtained from the boil-off calorimetric method.

3.4 Major sources of error in calorimetric investigation of multilayer insulations

Some possible sources of errors in the heat flux estimation using boil-off calorimetry have been discussed in Section 2.1. Apart from these, the major sources of errors in the estimation of effective thermal conductivity and heat flux are primarily due to (a) measurement errors (b) edge effect and lateral heat conduction.

3.4.1 Measurement errors

From the Fourier equation (1) of one dimensional heat transfer, the relative error components in the estimation of effective thermal conductivity of MLI can be expressed as

$$\Delta K_{eff} = \Delta Q + \Delta\delta + \Delta A + \Delta_{\Delta T}$$

where

ΔK_{eff} = relative error of estimating the thermal conductivity coefficient

$\Delta\delta$ = relative error of measuring the insulation thickness

ΔA = relative error in measuring the insulation surface area

$\Delta_{\Delta T}$ = relative error in measuring the boundary temperature difference.

According to Golovanov [23], the accuracy of measuring $\Delta\delta = \pm 3$ %, $\Delta A = \pm 0.3$ %, $\Delta_{\Delta T} \pm 0.1$ % and reasonably in the estimation of K_{eff}, the errors ΔA and $\Delta_{\Delta T}$ can be neglected. Error in the measurement of ΔQ is frequently the bigger source

of error and it can vary from ± 5 % to ± 30 % for different types of insulation and measurement conditions.
However the measurement errors reported by different authors for a variety of experimental systems differ substantially. For example Coston and Zierman [17] give the following figures in their experiments with a double guarded flat cold plate calorimeter.

$$\Delta Q = 5\ \%, \Delta\delta = 4\ \%, \Delta_{\Delta T} = 2\ \%\ (\Delta A \text{ is not given}).$$

The same authors, in the experiment with a double guarded cylindrical calorimeter has indicated that the major error is due to thickness measurement of the insulation and this alone can be ± 10 %.

Black et al. [24] has given the probable errors for a double guarded flat cold plate calorimeter as,

$$\Delta Q = 2\ \%, \Delta A = 4\ \%, \Delta\delta = 1\%, \Delta_{\Delta T} = 2\ \%$$

For a single guarded cold plate calorimeter, Black et al. [19] have given the probable errors as $\Delta Q = 1\ \%, \Delta A = 4\ \%, \Delta\delta = 1\ \%, \Delta_{\Delta T} = 2\ \%$.

De Hann [7] has estimated the errors for a small capacity tank calorimeter as,

$$\Delta Q = 6\ \%, \Delta\delta = 5 - 10\ \%.$$

The overall maximum errors reported by different authors in the estimation of K_{eff} are given in Table 1.

3.4.2 Error analysis in the estimation of K_{eff}

The uncertainties in the estimation of K_{eff} can be evaluated for the single sample experiment as given by Kline and Mc Clintock [25].

From equation (1) to (3)

$$K_{eff} = Q\delta/A\,(T_h - T_c)$$
$$Q = \dot{m}\,L_v$$
$$\dot{m} = \dot{V}\,\rho_o\,T_o\,P/T\,P_o$$

$$K_{eff} = \frac{\dot{V}\,\rho_o\,T_o \cdot P \cdot \delta \cdot L_v}{T \cdot P_o \cdot A \cdot (T_h - T_c)}$$

Putting $(T_h - T_c) = T_d$, $\dot{V} = V/t$, where V is the volume measured in time 't'.

$$\frac{\rho_o \cdot T_o \cdot L_v}{P_o} = \text{constant } C,$$

$$K_{eff} = \frac{C \cdot V \cdot P \cdot \delta}{t \cdot T \cdot A \cdot T_d} \tag{7}$$

The uncertainty $U_{K_{eff}}$ in the estimation of Keff can be expressed in terms of the uncertainties of the variables V, P, δ, T, A, t and T_d.

$$U_{K_{eff}} = \left[\left(\frac{\partial K_{eff}}{\partial V} \cdot U_V \right)^2 + \left(\frac{\partial K_{eff}}{\partial P} \cdot UP \right)^2 + \left(\frac{\partial K_{eff}}{\partial \delta} \cdot U_\delta \right)^2 \right.$$

$$+ \left(\frac{\partial K_{eff}}{\partial t} \cdot U_t \right)^2 + \left(\frac{\partial K_{eff}}{\partial T} \cdot U_T \right)^2 + \left(\frac{\partial K_{eff}}{\partial A} \cdot U_A \right)^2$$

$$\left. + \left(\frac{\partial K_{eff}}{\partial T_d} \cdot U_{T_d} \right)^2 \right]^{1/2} \tag{8}$$

The terms can be evaluated as:

$$\frac{\partial K_{eff}}{\partial V} = \frac{C \cdot P \cdot \delta}{t \cdot T \cdot A \cdot T_d} \tag{9}$$

$$\frac{\partial K_{eff}}{\partial P} = \frac{C \cdot V \cdot \delta}{t \cdot T \cdot A \cdot T_d} \tag{10}$$

$$\frac{\partial K_{eff}}{\partial \delta} = \frac{C \cdot V \cdot P}{t \cdot T \cdot A \cdot T_d} \tag{11}$$

$$\frac{\partial K_{eff}}{\partial t} = \frac{C \cdot V \cdot P \cdot \delta}{t^2 \cdot T \cdot A \cdot T_d} \tag{12}$$

$$\frac{\partial K_{eff}}{\partial T} = \frac{C \cdot V \cdot P \cdot \delta}{t \cdot T^2 \cdot A \cdot T_d} \tag{13}$$

$$\frac{\partial K_{eff}}{\partial A} = \frac{C \cdot V \cdot P \cdot \delta}{t \cdot T \cdot A^2 \cdot T_d} \tag{14}$$

$$\frac{\partial K_{eff}}{\partial T_d} = \frac{C \cdot V \cdot P \cdot \delta}{t \cdot T \cdot A \cdot T_d{}^2} \tag{15}$$

(For the estimation of the above terms, appropriate experimental data can be used in the right hand side terms).

Uncertainty intervals of different variables

(1) U_V = Uncertainty in the volumetric measurement using a flow meter (eg: integrated flow meter $\pm$ 100 cc).

(2) U_P = Uncertainty in the test chamber vapour pressure reading (eg: $\pm$ 5 Torr).

(3) U_δ = Uncertainty in the measurement of insulation thickness.

(4) U_t = Uncertainty in the measurement of time for flow measurement.

(5) U_T = Uncertainty in the temperature of the gas at the gas outlet of flow meter.

(6) U_A = Uncertainty in the estimated surface area of insulation.

(7) U_{T_d} = Uncertainty in the temperature measurement of both warm and cold boundaries

$$\left[\text{eg: } \begin{pmatrix} \pm\ 0.5\ K\ + \\ \pm\ 0.5\ K \end{pmatrix}\right] = \pm\ 1.0\ K$$

The percentage uncertainty in the estimation of K_{eff} is

$$= \frac{U_{K_{eff}}}{K_{eff}} \times 100 \tag{16}$$

3.4.3 Edge effect and lateral heat conduction

Theoretically, calorimetric estimation of heat flux in multilayer insulations assumes that the specimens are of infinite length and width but low enough in thickness, to assume a model for one dimensional heat transfer. However, in actual calorimetric experiments, the samples are of finite size and of some thickness such that the above assumptions are not truely valid. The heat transfer between the sample edges and the environment can cause a distortion in the temperature profile of the insulation layers near the edge boundaries as compared to the central area of the insulation. Thus the heat flux estimated becomes influenced by the lateral conduction caused by this temperature distortion and this is known as 'edge effect'.

What makes the 'edge effect' a significant factor in MLI investigations is its highly anisotropic characteristics. For MLI employing aluminium foil radiation shields of 6 μm thickness, a parallel to perpendicular conductivity ratio of 10^5 is typical, whereas this ratio is about 10^3 for aluminised Mylar shields. Because of the high order of anisotropy in the insulation, the temperature distortion at the edges of finite sized samples propagates fast much into the interior of the sample.

For the flat plate and cylindrical calorimeters, the insulation sample extends over the guard chambers so that the above distortion in the temperature profile tapers off for the measurement section. However, this itself is not often sufficient, when the insulation thickness exceeds a certain value. The effect of edge conduction and means to reduce it have been studied experimentally and analytically by several authors.

Golovanov [23] and Coston and Zierman [17] studied the effect of subjecting the sample edges to a edge shield at a temperature that of (i) cold boundary (ii) warm boundary (iii) an intermediate temperature between cold and warm boundary temperatures. It has been shown that for a flat plate calorimeter, the edge effect is minimized when the sample edges are shielded at an intermediate temperature between T_h and T_c. Alternately Coston and Zierman have suggested the use of an intermediary insulation of finite thickness at the outer edges of the sample to reduce edge effect. Black and Glaser [10] used a horizontal copper edge shield for this purpose. Halaczek and Rafalowicz [18] used a one mm gap between the test and guard sections of the insulation, ensured by a paper ring insert during assembly to reduce edge effect.

Caren and Cunnington [26], Coston and Zierman [17] and Getty et al. have studied edge effect for cylindrical calorimeters. The first two authors have suggested that the radiation shield should be terminated approximately 7 cm

shorter than the thermal spacer and the cryostat end. Additional cold end plates are to be used if the radiation shield is of aluminium foil. Getty et al. have shown that decrease in the lengths of the insulation over the guard sections can increase heat flux to the test section as much as by 28 %.

3.5 Comparison of calorimetric methods - cylindrical, flat cold plate, flat hot plate and tank calorimeters

Cylindrical and flat plate calorimeter can provide test data at fairly standardised conditions of insulation application and thus suited to compare performance of different types of insulations. However, their test geometries are not close enough to usual cryosystems on which insulation is to be applied. Tank calorimeters on the other hand are closer to the actual systems but it is rather difficult to achieve standard conditions. For example, the thickness of the insulation can vary at the cylindrical portion of the tank calorimeter to that at the dished ends due to insulation overlaps. Similarly the winding pressure or the compression can differ from one point to another of the tank surface.

In spite of the standardised conditions of applications, cylindrical and flat plate calorimeters suffer from edge effect and methods to offset them are not fully satisfactory. In the case of tank calorimeters, edge effect is absent, since the insulation covers the entire area. Between the cylindrical and flat plate calorimeters, edge effect is more critical in the latter, because for the same edge circumferential area, flat plate geometry gives less insulation surface area as compared to cylinder calorimeters. In other words for the same insulation test area, edge conduction is less for cylindrical profile. Golovanov [23] states that the relative measurement of the heat flux by a flat plate device is inversely proportional to half of the guard vessel diameter, whereas it is inversely proportion to double the lengths of the top and bottom guard chambers for a cylindrical calorimeter.

Flat plate calorimeters hold a distinct advantage over cylindrical calorimeters, when the heat flux has to be measured as a function of compressive load on MLI. Though the effect of local compression could be evaluated even on a cylindrical profile [28], precise measurement can be done only with a flat plate calorimeter.

Flat plate (vertical) calorimeters can provide test surface area much larger than flat horizontal calorimeters or cylindrical calorimeters and are comparable in that sense to tank calorimeters. However, they present the danger of larger edge effect.

Comparing the boil off calorimetric method (flat cold plate) and electrical input method (flat hot plate) Golovanov [23] indicates higher accuracy for the boil off method. According to him the accuracy in measuring the heat flux by electrical method is about ± 12 %. For flat cold plate the accuracy depends on the cryogenic fluid. It is ± 5 % for nitrogen, ± 4 % for parahydrogen and ± 2 % for helium.

SECTION 4: HEAT LEAK MEASUREMENT METHODS FOR CRYOCOMPONENTS AND TRANSFERLINES

4.0 Methods for heat leak measurement

Several methods could be used to measure heat leak through cryo-components such as supports, suspensions, couplings, transferlines etc. Often these techniques could be used to monitor the thermal performance of insulations as well. Some of the typical methods are:

(a) Measurement of the enthalpy change of the fluid flow
(b) Boil-off calorimetric method
(c) Thermal equilibrium method
(d) Cryogen transfer quantity measurement
(e) Heat meter method.

4.1 Measurement of enthalpy change of fluid flow

In this method to estimate the heat leak to a cryogen flow passage, a cold vapour at appropriate temperature is sent through the test passage equipped with temperature sensors at the inlet and outlet of test section and provision for mass flow measurement. Under steady state conditions, the enthalpy change gives the heat leak to the test system [29,30,31].

Ageyav [29] discussed the scheme for the estimation of heat leak into superconducting dipoles using helium vapour pressure thermometry. Fig. 4 shows the schematic of the heat leak test set up. Since the temperature difference estimated from the readings of two separate thermometrs will have an accuracy equal to the doubled limited accuracy of each thermometer, the authors have used a differential vapour pressure transducer to measure the temperature difference along the test section.

The heat flux $\dot{q} = \dot{m}\,(h_2 - h_1)$ (17)

where $\dot{m}$ = mass flow rate
h_1 = enthalpy of the fluid at inlet
h_2 = enthalpy of the fluid at outlet.

Hosoyama et al. [30] used germanium sensors for temperature measurement and gas flow meters for mass flow estimation.

4.2 Boil-off calorimetric method

The principle of boil-off calorimetry discussed under section 2.1, is valid for heat leak measurements also. Shibanuma et al. [32] have used the boil-off method to optimize insulation application methods for cryogenic pipelines and their test facility is shown in Fig. 5. Hakuraku et al. [33] estimated the heat leak through cryogenic supports of levitation magnets using a boil-off calorimeter shown in Fig. 6.

4.3 Thermal equilibrium method for estimation of heat leak to a cryogenic pipe

Blanchard et al. [34] have used this method to estimate the heat leak to a MLI insulated LN_2 pipe. The theory of the measurement method can be explained with the aid of Fig. 7. The outer vacuum tube of the multilayer insulated pipe is uniformly wound over with a heater and over that, an external insulation (foam) is provided to isolate the measurement surface from the environment. If the surface temperature of the outer wall is controlled such that it is in equilibrium with the environment of the test bath (shown in Fig. 8), then the heat leak through the test section of the pipe is equal to the heater power under steady state conditions.

4.4 Cryogen transfer quantity measurement method

Laeger et al. [35] and Blessing et al. [36] have used this method to evaluate the thermal performance of liquid helium transferlines. The experimental set-up identical in both the cases is shown in Fig. 9. Liquid helium is transferred from a dewar through the test line into a receiver cryostat, where the transferred liquid fraction is being evaporated by a feed back controlled heater, so as to keep the liquid level constant in the receiver cryostat. Measurements are taken in quasi-steady state conditions, by controlling the dewar and cryostat pressures so as to stabilize the transfer conditions. The mass flow rate of evaporation from the cryostat and the gas flow rate from the return line of the transfer line, heater power and gas outlet temperatures are measured continuously using a data acquisition system. Analysis of the data yields the heat flux to the transfer line.

4.5 Heat meter method

The basic principle of the heat meter technique has been briefly discussed in section 2.3

The technique of measurement of heat leak using a heat meter is not new. Earlier works reported include that of Kinzer and Pelanne, who estimated the thermal conductivity of some of the cryogenic insulation materials [14]. However, the non-availability of a reference material of low thermal conductivity closer to multilayer insulations had restricted its use for sometime. In the past 10 years, Fermi Laboratory has refined the heat meter technique to estimate the heat leak through cryogenic support systems and multilayer insulations [15, 37, 38, 39, 40, 41, 42]. They have made use of the NBS reference material 735 austenitic stainless steel, which has known thermal conductivity of 0.3 Wm^{-1} K^{-1} near 5 K and 8.1 Wm^{-1} K^{-1} near 79 K, as the heat meter element and effected a thermal conductance measurement.

The heat meter assembly is shown in Fig. 10 and Fig. 11. The thermally resistive stainless steel reference section is sandwiched between the thermally conductive copper threaded ends. For measurements down to liquid helium temperature, a pair of carbon resistors is used to sense the temperature accross the reference section and for measurements at LN_2 temperature and above, a pair of platinum sensors is used. A calibration heater is located at the warm end and the calibration is accomplished by measuring the output of the temperature sensors for different calibration heater power values. During the calibration run, the cold end of the heat meter is coupled to the cryogen reservoir while the warm is kept free (no sample attached) and the entire assembly is enclosed by a radiation shield at the cryogen reservoir temperature.

A typical cryostat developed in the Fermi Laboratories using the heat meter technique to estimate the heat leak through a magnet support system is shown in Fig. 12. The liquid helium vessel of 10.6 litre capacity provides the thermal sink for the test object through the heat meter. An external helium dewar of 26 litre capacity surrounds all but the lower end of the test vessel, thus reducing the heat load to the thermal sink reservoir. The boil off gas from the external helium dewar is used to cool down an intermediate temperature flange to a regulated temperature within 10 - 40 K. A 14.5 litre capacity LN_2 vessel with automatic refilling provision surrounds the external helium dewar and a 80 K shield from this vessel encloses the intermediate temperature shield. A bellow attachment to the vacuum chamber, with a regulated heater plate provides the 300 K surface

and enables to give a compressive load to the plate due to the differential pressure acting on the bellow.

The background heat leak to the facility has been estimated and the heat meter calibrated at both liquid helium and liquid nitrogen cold end tempreatures at the calibration heater power ranges of 0 - 0.250 W at 4.5 K and 0 - 3.0 W at 80 K. The measurement sensitivity is about 10 μW at liquid helium temperature and 10 mW at LN_2 temperature. The corresponding stabilization time for the heatmeter unit is 1 minute and 25 minutes at 4.5 K and 80 K respectively. The steady state conditions of measurement will depend on the time required for the sample to reach steady state.

4.6 Comparison of different methods for heat leak measurement

Each one of the methods discussed above may be better suited in a specific case over the others. However in general, the following are some of the merits and demerits of the different methods.

The measurement of enthalpy difference of the flow is one of the simplest means of measuring the heat leak and has the advantage that it involves single phase flow of vapour. The major difficulty of the method is that the temperature difference along the flow section is often very small for reasonable mass flow rates and conventional temperature sensors like carbon resistor do not give enough accuracy. The use of differential vapour pressure transducer [29] overcomes this defect to some extent. An alternate option is to decrease the mass flow rate to achieve higher temperature difference. But this results in a longer cool down time constant and increases possibilities for more perturbation in the system, preventing achieving equilibrium status for the flow. Lower flow rates also give rise to variation in the fluid temperature over the flow cross section and thus possible errors in temperature measurement.

Since the latent heat of vapourisation of cryogenic fluids is rather small and they have high ratio of vapour to liquid volume on evaporation, boil off calorimetry offers a very practical means to estimate even very small heat leaks. However, the general precautions to be taken in boil off calorimetry (section 2.3) measurements are essential for proper estimation of heat leaks.

The 'thermal equilibrium method' using controlled heating of the outer wall of a cryogenic pipe, requires an apparatus more complex than that for the enthalpy method or boil-off calorimetry method. This method involves complex temperature control techniques. The main advantage is that measurements are

required on the outer wall of the cryogenic line and thus a finished item or bought out cryogenic pipe lines could be tested. Further, the method offers some information over the variation of heat leak along the length of the pipe.

One of the main advantage of heat meter technique is that there is no need to mount temperature sensors on the test sample to measure the heat leak: they are mounted on the heat meter. As compared to boil-off calorimetry, heat meter method offers a few advantages (i) the data acquisition time is greatly reduced, since there is no need for the cryogen reservoir to reach equilibrium conditions - only steady state for the test sample is required (ii) atmospheric pressure variation has no measurable effect in this method and hence no pressure controllers are needed (iii) the resolution of measurement for the heat meter is in microwatts compared to milliwatts for gas meters used in boil-off calorimetry.

However, the heat meter method has also certain drawbacks. They include:

(i) corrections have to be made in the estimated heat leak, since the coldest spot of the sample under measurement is at the warm end of the heat meter and not at the temperature of the cryogen reservoir.

(ii) Even with a radiation shield connected to the cold end and the calibration procedure partially compensating for the infra red radiation, there is a finite amount of heat transfer, which is not compensated by the calibration procedure.

(iii) The heat meter technique is not suited for estimation of heat leaks for all possible configurations of test systems, e.g. heat leak estimation through a small diameter, long length pipe line, for which the boil-off method or the enthalpy difference methods are better suited.

(iv) The heat meter system is more complex and costly as compared to the boil off or the enthalpy difference methods.

SECTION 5: TEST FACILITIES FOR MULTILAYER INSULATION (1959 - 1992)

5.0 Need and scope for test facilities

The need for characterizing and optimizing thermal insulations, in particular multilayer insulation, received importance in the early phase of the above period due to the spurt in space programs whereas in the past one decade, it has been largely due to the fast growing needs for high energy physics devices. It is to be noted that the basic concepts of the test facilities to evaluate the thermal performance of insulations have remained mostly same except for better instrumentation and data acquisition systems. However due to better understanding of heat transfer mechanisms in MLI and the factors affecting its performance, better quality insulations and application techniques are being envolved with time. Even then there is a wide gap between theoretically possible insulation quality and the quality obtained in practice. Thus testing and optimizing the multilayer insulation remains a task of continuous interest and importance.

The principles of different measurement techniques to estimate the heat flux through MLI and the broad concepts of various calorimeters for that purpose have been already discussed in the previous sections. The following are the salient features of some of the representative types of test facilities built upto now at various laboratories in the world.

5.1.0 Cylindrical calorimeters

The general features of cylindrical calorimeters are discussed in section 3.1.

5.1.1 CEL-NBS calorimeter (77 - 300 K), 1959 [13]

This double guarded calorimeter has been shown in Fig. 1 and is the first cylindrical calorimeter used to evaluate the thermal performance of multilayer insulations. The basic parameters of this calorimeter designed and constructed at the Cryogenic Engineering Laboratory of the National Bureau of Standards, USA are given below:

(a) Test chamber:

diameter	$\simeq$	100 mm
length	$\simeq$	450 mm
volume	$\simeq$	2.3 litres
material	--	copper $\simeq$ 1.9 mm thick

(b) Guard chambers:

(i) upper guard:

diameter $\simeq$ 100 mm

length $\simeq$ 350 mm

(ii) diameter $\simeq$ 100 mm

length $\simeq$ 100 mm

Volume of guard chambers (top or bottom) $\simeq$ 3.5 litres

Material - copper $\simeq$ 1.9 mm thick

Test surface area $\simeq$ 0.14 m^2

Wet gas flow meter is used for flow estimation.

5.1.2 General Dynamics (300 - 20 K), 1965 [27]

The test calorimeter shown in Fig. 13 is more or less identical to the NBS calorimeter.

5.1.3 Lockheed Missiles and Space (300 - 4.2 K), 1967 [17]

The double guarded cylindrical calorimeter (Fig. 14) is modelled after the CEL-NBS calorimeter. However, this design has longer guard sections as compared to the NBS version, in order to reduce the effect of edge conduction. The dimensions of the test chamber are unaltered.

The schematic of the cryostat and associated instrumentation is shown in Fig. 15. Additional cooling shields are used for the top and bottom guard chambers, if the calorimeter is filled with LHe or LH_2. 6.5 mm diameter copper rods are mounted vertically inside the cryostat to reduce stratification of the fluid. A wet gas flow meter is used to measure boil off rate and a mercury column pressure controller is used to control the test chamber vapour pressure. Alfatron gauge was used to measure vacuum in the range 760 to 10^{-3} Torr, while an ion gauge was used for monitoring vacuum below 10^{-3} Torr.

5.1.4 Southampton University (300 - 77 K), 1974 [3]

A double guarded cylindrical calorimeter similar to CEL-NBS was used by Scurlock and Saull to evaluate the performance of carbon loaded glass paper, as a thermal spacer for MLI. The cryostat is shown in Fig. 16. The bottom guard of the

cryostat is provided with an activated adsorber packet, to improve vacuum levels in some experiments. The calorimeter was provided with a Penning gauge, a Pirani gauge, a gas bleed valve and a bursting disc. The gas flow measurements were taken using an integrated gas flow meter and periodically checked by collecting nitrogen over water column in a calibrated gas jar.

Insulation test area = 0.1015 m^2

5.1.5 Nippon Laboratories, Japan (300 - 77 K), 1980 [44]

A double guarded cylindrical calorimeter similar in construction and operation to the NBS calorimeter was used by Matsuda and Yashikiyo to evaluate the performance of special types of MLI with aluminium directly coated on one side of the thermal spacer. The vacuum level was measured using B - A gauge (10^{-1} - 10^{-5} Pa) and Pirani gauge ($< 10^{-1}$ Pa).

5.1.6 IHI Research Institute, Japan (300 - 4.2 K) 1986 - 1992 [11]

The double guarded cylindrical calorimeter, with a provision for an additional LN_2 top guard is used by Ohmori et al. to test dimpled MLI and is shown in Fig. 17 (a) and Fig. 17 (b).

The dimensions of the chambers differ from the CEL-NBS design. It appears that MLI is applied over the entire surface of the calorimeter test and guard chambers to avoid edge conduction. In the earlier versions, a teflon manostat was used to keep the pressure of the guard chamber higher than the test chamber and a soap flow meter was used for flow measurement. However, now two separate mass flow meter are used for flow measurement and the higher flow rate from the guard section itself provides the necessary differential pressures. The data acquisition system now comprises of a hybrid recorder with a IC memory chip and connected to a P.C. through a memory card reader and RS 232 C bus. The high vacuum is measured using a B - A gauge.

Approximate test area $\simeq$ 0.098 m^2

5.1.7 DESY, Hamburg (300 - 77 K), 1987 [45]

The calorimeter at DESY is a top guarded cylindrical calorimeter as shown in Fig. 18. The measurement cylinder has LN_2 pipes attached to the inner surfaces to provide thermosyphon action and the evaporation rate is measured using an inverted measuring jar (volumetric displacement system).

Insulation test area $\simeq$ 0.7 m^2

5.1.8 Mitsubishi Laboratories (300 - 77 K), 1988 [21]

Amano et al. have used a double guarded cylindrical calorimeter (Fig. 19) to study the relative merits of the roll type and the laminar type of insulation winding and to compare the performance obtained with a plat-in-box calorimeter. Mass flow meters were used to measure evaporation rate.

Surface area for test insulation $\simeq$ 0.5 m^2

5.1.9 TRIUMF, University of Victoria, Canada (300 - 4.2 K), 1985 -1988 [46,47]

A rather unusal profile, ie. flat rectangular shaped measuring and top guard chambers, was used by Gathright and Reeve to study MLI heat transfer especially in the 77 - 4.2 K range. The indium sealed vacuum jacket is immersed in LN_2 to provide the 77 K boundary. Rotameters and integrated gas flow meters were used for flow measurements.

Surface area of test chambers $\simeq$ 0.033 m^2

5.1.10 IISc, Banglore, India (300 - 77 K) 1989 [48]

A double guarded cylindrical calorimeter shown in Fig. 20 was used to evaluate the performance of indigeneous MLI comprising double aluminized Mylar and nylon net. The dimensions are comparable to that of Lockheed calorimeters (5.1.3). The test chamber is of copper but the guards are of stainless steel lined inside with copper mesh. Integrated flow meter is used for flow measurement.

Test surface area $\simeq$ 0.14 m^2

5.2.0 Flat plate calorimeters

General features of flat plate calorimeters are discussed in section 3.2. The following are some of the typical flat plate test facilities.

5.2.1 ADL.Inc., USA (300 - 77 K), 1959 [19]

The first cold flat plate apparatus to measure the thermal effectiveness of MLI developed by Black et al. is shown in Fig. 21. It comprises of a test chamber of $\simeq$ 70 mm diameter and 1/2 litre capacity, enclosed except at the base by a guard chamber of $\simeq$ 150 mm diameter and 5.25 litres capacity.

Insulation test area $\simeq$ 38.5 cm^2

5.2.2 ADL. Inc., USA (533 - 4.2 K), 1963 [10, 24]

This double guarded flat plate calorimeter was a versatile one designed to evaluate multilayer insulation under varying test conditions including mechanical compression (0 - 50 psi). The calorimeter features are shown in Fig. 22. The guarded cold plate consists of a measuring vessel 150 mm in diameter and 2.5 litre capacity. Leaving the flat bottom cold plate, it is enclosed by a 300 mm diameter guard chamber of 27 litre capacity. The warm plate position can be varied by an external operation of a hydraulic piston to provide mechanical compression of the sample. For experiments down to 4.2 K, the test and inner guard are further shielded by an external guard filled with LN_2. The barometric pressure variation effects are controlled by a mercury column device and the evaporating gas flow rate is measured by an automatic volume displacement measurement technique.

Insulation test area $\simeq$ 175 cm^2

5.2.3 Lockheed laboratories, USA (300 - 20 K), 1964 [17]

This flat cold plate calorimeter is fairly similar to the one described in 3.2.The mass flow rate is measured by a Schuco mass flow meter.

Insulation test area $\simeq$ 175 cm^2

5.2.4 High energy laboratory, Dubna (293 - 20 K), 1968 [23]

This is a combined flat hot and cold plate calorimeter (Fig. 23) built to compare the boil-off method and the electrical input method in the heat flux estimation of MLI.

No dimensional details are available.

5.2.5 Fermi laboratory, USA (277 - 4.2 K), 1979 - 86 [9, 20, 49, 50]

This is a flat cold plate calorimeter with a difference; instead of a flat horizontal plate, it has a flat vertical plate enclosed inside a rectangular box [Plate-in-Box calorimeter].

The schematic of the calorimeter system is shown in Fig. 24(a). The cooling of the copper plate is achieved by thermosyphon effect and this copper tube is connected to the inner helium vessel through a coupling. The inner helium test vessel is guarded by an external helium guard vessel and radiation shields, which in turn are shielded by a nitrogen guard vessel and radiation shield. The 77 K boundary temperature is obtained for the box by a connection to the liquid nitrogen reservoir and is insulated on the outside by MLI. The flow measurement is done with a wet gas flow meter together with a chart recorder. The vacuum is monitored using a Philips ion gauge.

The same calorimeter has been used later for investigations in the (277 - 77 K) range [20]. Further instrumentation were incorporated such as heater and control circuit, fast warm up gas circuit, provision for gas bleeding and vacuum level control. Vacuum was measured using a cold cathode gauge. The schematic of the experimental system is shown in Fig. 24(b).

Insulation test area $\simeq$ 2.26 m^2

5.2.6 Institute for low temperature and structural research, Poland (295 - 87K), 1985 [51]

The hot plate calorimeter is shown in Fig. 25. In this calorimeter, the cold boundary temperature is obtained through a cold finger connected to the liquid nitrogen reservoir and the temperature of the cold finger can be changed with electrical heating. The measurement plate has a 400 Ω manganin heater to allow estimation of the heat flux and the plate is shielded by a guard plate heater

arrangement. Edge effects are controlled by using a ring section of the insulation around the test sample with a 1 mm gap between them.

Insulation test area $\simeq$ 78 cm^2

5.2.7 Institute for low temperature Physics and Engineering, Kharkov (300 - 77K), 1985 [52]

At Kharkov, mostly flat hot plate calorimeters are used for MLI investigations. A schematic of a typical system is shown in Fig. 26.

Approximate test area $\simeq$ 200 cm^2

5.2.8 Mitsubishi Laboratories (77 - 300 K), 1988 [21]

A vertical cold plate calorimeter (Plate-in-Box) used at Mitsubishi laboratories is shown in Fig. 27. The plate cooling is obtained with thermosyphon effect.

Test surface area $\simeq$ 1.55 m^2

5.3.0 Tank calorimeters

The general features of tank calorimeters have been discussed under section 3.3. Various test facilities employing tank calorimeters are listed below.

5.3.1 Cryogenic engineering. Co., USA (300 - 4.2 K), 1964 [7]

One of the first calorimeters which can be called as tank calorimeter was used by De Hann and is shown in Fig. 28. The apparatus was designed as an easily demountable dewar with provision for using a variety of cryogenic fluids. Further, different capacity inner vessels could be used for the standard outer vessel. The boil off was measured using a wet gas flow meter.

Typical test surface area $\simeq$ 0.6 m^2

5.3.2 ADL, USA (300 - 77/4.2 K), 1966 [53]

The tank calorimeter used in ADL has been already discussed in section 3.3 and shown in Fig. 3. This was one of the first tank calorimeters designed for optimizing MLI application technique on large capacity tanks.

The calorimeter is about 1.2 metre in diameter and 70 cm deep. It is suspended inside a vacuum chamber about 1.5 metre in diameter and 2.25 m high. The test tank was enclosed by two split radiation shields of copper and is provided with integral cooling coils.

Test surface area $\simeq$ 3.7 m^2

5.3.3 Lockheed Research Laboratories [T_h = 295 - 80 K, T_c = 135 - 15 K], 1984 [54]

Nast et al. have made a tank calorimetric study of multilayer insulations with variable warm and cold boundary temperatures. A schematic of the calorimeter is shown in Fig. 29. The 280 litre capacity 6061 aluminium test tank is filled with 1.8 % density foamed aluminium to provide isothermal conditions. To reduce background heat leaks, the tank is suspended by a bundle of 19 dacron fibres and the fill and vent line are of convoluted teflon tubing. The warm boundary is a 1.2 mm thick aluminium shield cooled by a two-stage cryorefrigerator to the desired temperature and controlled by a temperature controller.

The flow rates are measured using a Hastings mass flow meter and two precision wet gas meters, all in series. Vacuum measurement is done using an ionisation gauge and a Baratron capacitance pressure sensor.

Test surface area $\simeq$ 2.38 m^2

5.3.4 Lockheed Research Laboratories [T_h = 295 - 30 K, T_c = 77 - 4.2 K], 1986 [55]

A small capacity (15 litres) tank calorimeter was made in which the outer warm boundary temperature could be as low as 30 K and the inner tank could be filled with LN_2 or LHe. The dewar was suspended using an FRP tube, with a stainless steel sleeve overlapped to prevent helium diffusion to the vacuum space. Mass flow measurement was done with a Matheson mass flow meter and wet gas meter in series.

Test surface area $\simeq$ 0.32 m^2

5.3.5 Institute for low temperature and structural research, Poland (250 - 77K), 1986 [18]

A 15 litre capacity demounable stainless steel tank calorimeter (Fig. 30) has been used to compare MLI performance with that obtained from flat plate calorimeter. A perforated copper screen is fixed around the inner tank, over which the insulation is applied.

Surface area $\simeq$ 0.3 m^2

5.3.6 KfK (292 - 77 K), 1988 [56]

A rectangular stainless steel tank (276 litre capacity) was used to evaluate NRC type MLI with carbon loaded glass paper as thermal spacer. Since the test specimens were suspended on the vertical plane of the tank, the configuration is essentially that of a plate calorimeter. The schematic of the test rig is shown in Fig. 31.

Test surface area $\simeq$ 2 x 2 m^2

5.3.7 KfK (300 - 77 K), 1988 [28]

In order to test blanket type of multilayer insulation the test stand "TESSI" shown in the Fig. 32 has been used. The test tank, cylindrical in shape (320 mm ∅ x 1900 mm length) and made of 2 mm thick copper, is housed inside a vacuum chamber 3.7 meter high and 1.5 m in diameter. The test surface is cooled down to liquid nitrogen temperature by thermosyphon effect and the heat flux is estimated from the boil-off measurements using a Hastings mass flow meter and integrated gas flow meter. A liquid nitrogen guard chamber and shielding reduces the external heat flux to the measuring chamber.

Test surface area $\simeq$ 2 m^2

5.4.0 Heat meter facilities

The use of a heat meter to measure the heat leak to cryogenic systems and in particular, the facility at Fermi laboratories had been discussed under section 4.5. The Heat Leak Test Facility (HLTF) of Fermi laboratory shown in Fig. 12 has been

specifically modified to evaluate candidates of the multilayer insulations for the superconducting magnets of the Super Collider, as given below.

5.4.1 Fermi laboratory (300 - 4.2 K), 1985 - 1992 [38, 39, 40, 41, 42]

The modified heat leak facility to evaluate multilayer insulation is shown in Fig. 33. The insulation test areas are provided by the side and bottom areas of a cylindrical OFHC cold plate, connected to the cryogen reservoir via the heat meter unit. The cold plate is 394 mm in diameter and 305 mm in height. A temperature controlled hot plate, also of copper, lines the functional end vacuum can and is separated from it by insulating liners. To limit thermal radiation to the cold plate from sources other than the hot plate, a guard plate at 80 K is employed. Thermal communication between the cold plate and the guard plate is reduced by some layers of multilayer insulation. The test facility has been recently modified [42], to vary the cold boundary temperature from 10 K - 40 K. The vacuum mesurements are by Bayard-Alpert gauge for high vacuum and thermocouple gauges for rough vacuum. The insulation layer temperatures are measured using cryogenic linear temperature sensors (CLTS).

$$\text{Test surface area} \simeq 0.5 \text{ m}^2$$

5.5.0 Comparison of test facilites

The comparison between various calorimetric techniques have been already made under section 3.5 and that of heat leak measurements under section 4.6. They are relevant for test facilities as well, employing these methods. However, they are not further discussed in detail in this section. But the following points are noted.

(1) The basic design and other features of cylindrical and flat plate (horizontal) calorimeters have remained the same for the past 30 years.

(2) The test surface area provided by cylindrical and flat plate (horizontal) are rather modest. Typically, cylindrical calorimeters have test surface area ranging from 0.1 - 0.7 m^2 whereas flat plate (horizontal) calorimeters have the smallest area ranging from 38 cm^2 - 200 cm^2.

(3) A relatively new concept in flat plate (vertical) or plate-in-box calorimeter was introduced by Fermi laboratory in 1979 [9], with the cooling of the plate by thermosyphon mechanism. Vertical plate calorimeters up to now have test surface area ranging from 1.55 m^2 to 2.26 m^2.

(4) Tank calorimeters simulate actual conditions of application of multilayer insulation on real systems better than any other facilities. They have typical surface areas ranging from 0.3 m^2 to 3.7 m^2.

(5) The flat plate calorimeters are more prone for errors in measurement due to higher edge conduction as compared to cylindrical calorimeters, whereas for tank calorimeter this effect is nearly absent.

(6) For a mid-size test facility with relatively large test area, only the flat vertical plate or tank calorimeter are available as on now.

(7) The method of heat meter evaluation was employed for multilayer insulations only in 1985 [38]. The first facility of this kind has been in the Fermi laboratory, which has a test surface area of 0.5 m^2.
Recently, heat leak measurements down to 1.8 K of cryogenic components using heat meter technique have been reported from CERN, Geneva [68]. The cryostat has provision to cross check the heat meter measurement using boil-off calorimetry.

(8) So far the heat leak facility at Fermi laboratory is the only multifacial facility capable of heat leak estimation for cryogenic components and MLI.

(9) Most of the heat flux measurements have been done using (a) wet gas flow meters (b) dry gas flow meters (c) mass flow meters. Rarely other techniques such as volume displacement measurement methods are used. The recent trend has been the use of mass flow meters.

(10) For high vacuum measurement, most of the investigators used Bayard-Alpert gauges while some of them used cold cathode (Penning) or Baratron (capacitance) gauges. For rough vacuum measurement Pirani or thermocouple gauges are widely used.

(11) For insulation layer temperature measurements most commonly used sensors are, copper-constantan thermocouples (300 - 77 K), platinum sensors (300 - 77 K), gold-iron thermocouple (77 - 4.2 K) and CLTS (300 - 4.2 K).

(12) There are only limited experiments done so far for heat flux estimation in MLI in the 77 - 4.2 K range. They are (i) Fermi laboratory using flat plate (vertical) calorimeters [9, 49] (ii) IHI, using double guarded cylindrical calorimeter [11] (iii) Lockheed, using tank calorimeter [55] and (iv) Victoria University, using rectangular profile calorimeter [46 and 47]. The experimental results from the heat leak facility using heat meter at Fermi laboratory is not yet available for the 77 - 4.2 K range.

(13) The data available so far from calorimetric measurements indicate that taping the thermal radiating surfaces with 3 M, No: 425 aluminium tape is the best way to reduce heat flux in cryogenic systems in the 77 - 4.2 K range as compared to MLI with thermal spacers. Spacerless MLI such as NRC-2 type or Dimpled MLI appears to be candidates for further evaluation.

(14) It should be acknowledged that useful data for the 77 - 4.2 K range is also, most likely to be found in studies related to space applications. However they are not covered in this report.

Appendix 1:

A new look at the performance indicator for MLI - heat flux vs. effective thermal conductivity

While for the past 30 years, the apparent or effective thermal conductivity (K_{eff}) has been in use as a relative performance indicator for different multilayer insulations, there have been some doubts whether this is rather a misleading conception. As early in 1966, Adelberg [57] showed that possible errors can be made with the misconception that K_{eff} is a material property. Gonczy et al. [41] in 1990 suggested using (heat flux x no. of radiating surfaces) as a more precise method to compare performance of multilayer insulations.

Due to the non-linear temperature profile in MLI, resulting from the presence of the radiation component along with the conduction components, the term "effective or apparent thermal conductivity" has been intented as a performance indicator or as a mean to compare different MLIs rather than a material property. However, a look at the summary of calorimetric data given in Table 2, shows that even for this purpose K_{eff} is not useful. For example, the well known data of Scurlock and Saull [3], a typical K_{eff} value for carbon loaded spacer insulation is 0.077 μW/cm-K, which is very close to the theoretical limit imposed by radiative heat transfer for floating shields. However, the heat flux data for the same Keff value shows a reasonable value of 0.517 W/m^2. Taking a more recent example from the Fermi lab paper [41], dimpled insulation of 26 layers gives a normal value of heat flux, 0.69 W/m^2 whereas the estimated K_{eff} value is 0.16 μW/cmK, which is one of the lowest reported after that of Scurlock. The rather low value of the insulation thickness has been the primary reason for the very low value of K_{eff} and the effect of error in the exact determination of thickness becomes more important in these cases.

A closer look at the compiled data from the various investigations (Table 2), reveals a better correlation between number of layers, boundary temperatures, vacuum level and other material data with respect to the heat flux as compared to K_{eff} values. Further, the heat flux data is able to indicate (300 - 7 7 K) and (77 - 4.2 K) regimes of heat transfer more distinctly than the Keff values. For example, taking the data from Ohmori et al. [11] and estimating some of the parameters, yield the following values:

Insulation	no: of layers	Layer density	$T_h - T_c$	Heat flux	K_{eff}
IHI-DI-DAM	40	4.02/mm	(293 - 77 K)	0.3 W/m^2	1.43×10^{-7} W/cm-K
- do -	- do -	- do -	(77 - 4.2 K)	0.052 W/m^2	0.79×10^{-7} W/cm-K

Thus the heat flux data shows a 5 fold reduction in heat flux whereas the K_{eff} value has just about 2 fold reduction for the same insulation between two different temperature ranges.

Further, the error margin in K_{eff} values are bound to be much larger than for the heat flux. A look at the equation (1) shows that, the errors probable in K_{eff} values not only include the errors of heat flux but also that in the measurement of thickness and boundary temperatures. Therefore heat flux can represent the MLI performance at a much reduced probability of error than K_{eff}.

However, the suggestion of Gonczy et al. [41] that heat flux x no. of radiating surfaces = constant is probably not true. This is because after an optimum number of layers, the heat flux reduction is not proportional to the number of layers but in fact can show an increase [39, 58] after an optimum number of layers, due to increased interlayer gas pressure, deviation from one dimensional heat transfer etc.

Therefore heat flux appears to be a more representative quantity as a performance indicator than effective thermal conductivity, (K_{eff}). However, there is a continuing need to specify the associated parameters of measurement such as test area, number of layers, layer density, boundary temperatures, vacuum levels etc. along with the heat flux data. In addition, the heat flux data should specify, whether it is related to experiments done using a standard test facility or any other cryogenic equipment. In the former case, it is to be known (a) the type of test facility (b) whether it is guarded or unguarded. If the data pertains to a cryoequipment, the method of insulation application and the joining techniques are to be specified.

Appendix 2:

Some critical factors affecting MLI performance

It is obvious that basic parameters such as number of layers, boundary temperatures etc. have significant effect on the performance of multilayer insulations. However, there are a variety of factors which may not be as apparent as the above parameters, nevertheless can be very significant. Some of these aspects are briefly mentioned.

(1) Coating thickness

The skin depth for black body radiation in aluminium is about 1000 Å [3]. Thus for coated films like aluminised Mylar, where the coating thickness is rarely of this order, it results in higher emissivity values. Ruccia and Hinkley [59] and Ohmori et al. [11] have studied this aspect in detail. A coating thickness less than 400 Å per side is not acceptable for aluminised Mylar due to the exponential increase in emissivity at lower coating thickness.

(2) Others factors causing higher emissivity

Even with good coating thickness or even for aluminium foil, there are factors which will adversely affect the emissivity in multilayer insulation.

(a) Mechanical handling

Any mechanical handling causing distortion of crystal structure can increase the radiation absorptivity. Thus crinkling of films after coating or that of aluminium foil can increase radiative influx. (For the same reason, mechanical buffing results in a optically bright but thermally dull surface for the cryovessel surfaces.)

(b) Surface oxidation

Surface oxidation can drastically change the emissivity value, except for aluminium because thin layer of aluminium oxide is transparent to infrared radiation [59]. However, copper and silver surfaces are adversely affected. Protective coatings increase the emissivity. Fixing aluminium tape over oxidised surface is a good solution [9, 20].

(c) Effect of the thermal spacer

It has been shown that the emissivity of a reflector (double aluminized Mylar, 800° A) is increased by a factor of 3.4 by introducing a thermal spacer

(200 μm thick polyester net) [66]. Carren and Cunnington [26] have suggested that a spacer should have a high radiation scattering cross section. Mikhalchenko et al. [52] have shown that transition from a scattering spacer to an absorbing one, not only increases radiative heat transfer but also solid conduction in some cases. Thus dimpled spacer free aluminized Mylar with good coating thickness can be a good performer [11, 41].

(d) Condensation of vapour

The quality of the vacuum and the composition of the outgassing species will have not only influence on the gas conduction heat transfer but also on radiative and solid conduction heat transfer [61]. It is well known that in many instances, the predominant outgassing species from MLI is water vapour and condensation of this on the shield can increase the emissivity drastically. Backstreaming of vacuum pump oil vapour is another source.

(3) Compression of insulation

The increased heat transfer due to compression in MLI is well known [22]. Even the self weight of the insulation can increase the heat flux through MLI [62].

(4) Effect of pre-conditioning temperature

It has been shown experimentally that the long time outgassing rate of aluminized Mylar is dependent on the pre-conditioning temperature [63]. The optimum pre-conditioning temperature for double aluminized Mylar is in the range of 343 - 363 K, above which the long term outgassing rate is shown to have increased.

(5) Method of wrapping

Roll type refers to continuous winding of insulation whereas, laminate type refers to separate layers of insulation of length equal to π x diameter, at each section.

Amano et al. [21] has shown that the laminate method of winding can reduce heat flux by 20 - 30 % as compared to roll type winding, due to the reduced longitudinal heat transfer component in this case. Improved laminate winding method is suggested by Shibanuma et al. [32].

(6) Interlayer gas pressure

The value of the gas pressure within the insulation can be 1 to 2 orders high as compared to the chamber vacuum, for specific conditions [64, 65, 66]. Thus increase in the number of layers can cause higher interlayer pressure, which not only nullify the reduction in radiation heat transfer expected but increase the overall heat transfer rate, for number of layers exceeding an optimum number. This may depend on boundary temperature, and pumping paths etc.

(7) Cracks and penetrations

The heat flux through a crack in MLI can be as high as $\simeq$ 150 W/m^2 [50] in the 300 - 77 K range, while it can be about $\simeq$ 180 mW/m^2 in the 77 - 4.2 range [49]. Thus the heat flux through a crack is more than one order higher as compared to the crack less insulation. Patch techniques can be effectively used to reduce the effect of cracks [50]. Insulation blanket joint configurations also need to be optimised [41].

Penetrations, in general, distorts the normal temperature profile in multilayer insulations and thus cause increased heat flux [4]. On the other hand they provide additional pumping paths and thus reduce interlayer gas pressure. The adverse effect of penetrations can be reduced by special insulation procedures at the penetration area [67].

(8) Thermal spacer properties

Apart from the radiative properties of the spacer which have been already discussed, several other parameters are important to reduce conductive heat transfer. They include the fiber diameter, mesh size, whether woven or non-woven etc. Also organic binders and basic outgassing charcteristics play an important role.

Concluding remark

This study of reference literature has been used for the following steps in realization of modification of the existing TESSI test facility:

- evaluation of the published datas and results and examination of their applicability for the modified TESSI test facility "THISTA"
- proposal of a concept and layout of the THISTA facility in terms of design, process engineering and measurement technique as a versatile KfK/ITP test facility for thermal insulation investigations in cryogenics (KfK-Primärbericht).

References

1 Kropschot, R.H., Schrodt, J.E., Fulk, M.M. and Hunter, B.J. Multi-layer insulation. Adv. Cryog. Eng. (1959) 5 189-198.

2 Halaczek, T.L. and Rafalowicz, J. Temperature variation of thermal conductivity of self-pumping multilayer insulation. Cryogenics (1986) 26 544-546.

3 Scurlock, R.G. and Saull, B. Development of multilayer insulation with thermal conductivities below 0.1 μW cm^{-1} K^{-1}. Cryogenics (1976) 303-311.

4 Murray, D.O. Degradation of multilayer insulation systems by penetrations. Adv. Cryog. Eng. (1967) 13 680-689.

5 Gibbon, N.C., Matsch, L.C. and Wang, D.I-J. Thermal conductivity measurements of insulating materials at cryogenic temperatures. Am. Soc. Testing Materials, Baltimore (1967) STP 411 61-73.

6 Kaganer, M.G. Thermal insulation in cryogenic engineering. Israel Program for Scientific Translations, Jerusalem (1969) 164.

7 De Hann, J.R. Thermal conductivity measurements of insulating materials at cryogenic temperatures. Am. Soc. Testing Materials, Baltimore (1967) STP 411 95-109.

8 Kaganer, M.G. Thermal insulation in cryogenic engineering. Israel Program for Scientific Translations, Jerusalem (1969) 161.

9 Leung, E.M., Fast, R.W. Hart, H.L. and Heim, J.R. Techniques for reducing radiation heat transfer between 77 and 4.2 K. Adv. Cryog. Eng. (1979) 25 489-499.

10 Black, I.A. and Glaser, P.E. The performance of double-guarded cold-plate thermal conductivity apparatus. Adv. Cryog. Eng. Eng. (1963) 9 52-63.

11 Ohmori, T., Tsuchiya, M., Taira, T. and Takahashi, M. Multilayer insulation with aluminized dimpled polyester film. Proc. ICEC-11 (1986) 567 - 571.

12 Karp, G.S. and Lankton, C.S. Thermal conductivity measurements of insulating materials at cryogenic temperatures. Am. Soc. Testing Materials Baltimore (1967) 13-24.

13 Mikhalchenko, R.S., Getmanets, V.F., Pershin, N.P. and Batozskii, Yu. V. Thermal insulation compositions for Cryogenic vessels with flexible impenetrable jacket. Proc. ICEC-10 (1984) 668-671.

14 Kinzer, G.R. and Pelanne, C.M. Thermal conductivity measurements of insulating materials at cryogenic temperatures. Am. Soc. Testing Materials Baltimore (1967) 110-118.

15 Kuchnir, M. Apparatus to measure thermal conductance. Cryogenics (1980) 203-207.

16 Burgess, W. and Lebrun, Ph. Compared performance of Kapton and Mylar based Superinsulation. Proc. ICEC-10 (1984) 664-667.

17 Coston, R.M. and Zierman, C.A. Thermal conductivity measurements of insulating materials at cryogenic temperatures. Am. Soc. Testing Materials (1967) STP 411 25-42.

18 Halaczek, T.L. and Rafalowicz, J. Heat transfer in self-pumping multilayer insulation. Cryogenics (1986) 26 373-376.

19 Black, I.A., Wechsler, A.E., Glaser, P.E. and Fountain, J.A. Thermal conductivity measurements of insulating materials at cryogenic temperatures. Am. Soc. Testing Materials (1967) STP 411 74-94.

20 Shu, Q.S., Fast, R.W. and Hart, H.L. Heat flux from 277 to 77 K through a few layers of multilayer insulation. Cryogenics (1986) 26 671-677.

21 Amano, T., Ohara, A. and Yamada, T. Effects of a radiation system and a wrapping method of multilayer insulation on heat transfer in cryogenic systems. Proc. ICEC-12 (1988) 162-166.

22 Black, I.A. and Glaser, P.E. Effects of compressive loads on the heat flux through multilayer insulations. Adv. Cryog. Eng. (1965) 11 26-34.

23 Golovanov, L.B., Measurement of thermal conductivity coefficient of multilayer insulations. Proc. ICEC-2 (1968) 117-122.

24 Black, I.A., Glaser, P.A. and Perkins, P. Thermal conductivity measurements of insulation materials at cryogenic temperatures. Am. Soc. Testing Materials, Baltimore (1967) STP 411 52-60.

25 Kline, S.J., and Mc Clintock, F.A. Uncertainty estimation in single sample experiments. Mech. Eng. (1953) 3 75-78.

26 Caren, R.P. and Cunnington, G.R., Advances in Cryogenic heat transfer, Am. Inst. Chem. Engineers (1968) 64 67-81.

27 Getty, R.C., Clay, J.P., Kremzier, E.J., and Leonhard, K.E. Experimental evaluation of some selected light weight superinsulation for space vehicles. Adv. Cryog. Eng. (1965) 11 35-48.

28 Barth, W., Lehmann, W., Henry, C. and Walter, R. Test results for a high quality industrial superinsulation. Cryogenics (1988) 28 607-609.

29 Ageyev, A.I., Levin, M.V., Logachev, S.N., Shamichev, A.V. and Zinchenko, S.I. Static heat leak measurements for UNK superconducting dipoles. Adv. Cryog. Eng. (1991) 37A 573-576.

30 Hosoyama, K. et al. A liquid helium transfer line system for superconducting RF cavity. Adv. Cryog. Eng. (1985) 31 1027-1034.

31 Laeger, H., Labrun, Ph. and Rohner, P. Long flexible transferlines for gaseous and liquid helium. Cryogenics (1978) 659-662.

32 Shibanuma, K. et al. Development of multilayer insulatior round internal pipes for JT-60 NBI Cryopumps. JEARI-M85-167 (1983).

33 Hakuraku, J. et al. Thermal performance of a low heat leak support for superconducting magnetic levitated trains. Proc. ICEC-9 (1982) 107-110.

34 Blanchard, E.R., Kirk, B.S. and Reiter, S.H. A technique for determining the local heat leak into a cryogenic pipe. Adv. Cryog. Eng. (1965) 11 631-637.

35 Blessing, H., et al., Four hundred meters of flexible cryogenic helium transferlines. ICEC-8 (1980) 261-

36 Blessing, H., Lebrun, Ph. and Schippl, K. Very low-loss liquid helium transfer with long flexible cryogenic lines. Adv. Cryog. Eng. (1990) 909-916.

37 Kuchnir, M., Gonczy, J.D. and Tague, J.L. Measuring heat leak with a heatmeter. Adv. Cryog. Eng. (1985) 31 1285-1290.

38 Gonczy, J.D. et al. Heat leak measurement facility. Adv. Cryog. Eng. (1985) 31 1291-1298.

39 Ohmori, T. et al. Thermal performance of candidate SSC magnet thermal insulation systems. Adv. Cryog. Eng. (1987) 33 323-331.

40 Boroski, W.N., Gonczy, J.D. and Niemann, R.C. Thermal performance measurements of a 100 percent polyester MLI system for the super-conducting super collider; Part 1: Instrumentation and experimental preparation (300 - 80 K). Adv. Cryog. Eng. (1990) 35 487-496.

41 Gonczy, J.D., Boroski, W.N. and Niemann, R.C. Thermal performance measurements of a 100 percent polyester MLI system for the super-conducting super collider; Part II: Laboratory tests (300 K - 80 K). Adv. Cryog. Eng. (1990) 35 497-505.

42 Boroski, W.N., Kunzelman, R.J., Ruschman, M.K. and Schoo, C.J. Design and calibration of a test facility for MLI thermal performance measurements below 80 K. Adv. Cryog. Eng. (1992) 37 A 275-283.

43 Hnilicka, M.P. Engineering aspects of heat transfer in multilayer reflective insulation and performance of NRC insulation. Adv. Cryog. Eng. (1959) 5 199-208.

44 Matsuda, A. and Yoshikiyo, Simple structure insulating material properties for multilayer insulation. Cryogenics (1980) 135-138.

45 Burmeister, H. et al. Test of multilayer insulations for the use in the superconducting proton-rig of Hera. Adv. Cryog. Eng. (1987) 33 313-322.

46 Gathright, T.R. and Reeve, P.A. Effect of multilayer insulation on radiation heat transfer from 77 K to 4.2 K. Proc. 9th Int. Conf. on Mag. Techno (1985) 695-699.

47 Gathright, T.R. and Reeve, P.A. Effect of multilayer insulation on radiation heat transfer at cryogenic temperatures, IEEE Trans. on Magnetics, 1988 (24) 1105-1108.

48 Jacob, S., Kasthurirengan, S. and Karunanithi, R. Investigations into the thermal performance of multilayer insulation (300 - 77 K). Part 1: Calorimetric studies. Cryogenics (1992) 1137-1146.

49 Shu, Q.S., Fast, R.W. and Hart, H.L. Crack covering patch technique to reduce the heat flux from 77 K to 4.2 K through multilayer insulation. Adv. Cryog. Eng. (1987) 33 299-304.

50 Shu, Q.S., Fast, R.W. and Hart, H.L. Theory and technique for reducing the effect of cracks in multilayer insulation from room temperature to 77 K. Adv. Cryog. Eng. (1987) 33 291-298.

51 Halaczek, T. and Rafalowicz, J. Flat-plate cryostat for measurement of multilayer insulation thermal conductivity. Cryogenics (1985) 25 593-595.

52 Mikhalchenko, R.S., Getmanets, V.F., Pershin, N.P. and Batozskii, Yu.V. Theoretical and experimental investigations of radiative-conductive heat transfer in multilayer insulation. Cryogenics (1985) 25 275-278.

53 Ruccia, F.E. and Hinckley, R.B. Thermal performance of tank applied multilayer insulations. Adv. Cryog. Eng. (1966) 12 218-228.

54 Nast, T.C., Naes, L. and Stevens, J. Thermal performance of tank applied multilayer insulation at low boundary temperatures. Proc. ICEC-10 (1984) 586-593.

55 Nast, T.C., Frank, D.J. and Spradley, I.E. Investigations of multilayer insulations at low boundary temperatures. Proc. ICEC-11 (1986) 561-566.

56 Barth, W. and Lehmann, W. Experimental investigations of superinsulation models equipped with carbon paper. Cryogenics (1988) 28 317-320.

57 Adelberg, M. Effective thermal conductivity and multilayer insulation. Adv. Cryog. Eng. (1966) 12 252-254.

58 Inai, N. Investigations of multilayer insulation. Heat Transfer-Jpn.Res. (1978) 7 61-73.

59 Ruccia, F.E. and Hinckley, R.B. The surface emittance of vacuum-metallized polyester film. Adv. Cryog. Eng. (1965) 11 300-307.

60 Saho, N. and Takada, T. Thermal characteristics of multilayer insulation. Proc. ICEC-9 (1982) 572-575.

61 Karskaya, T.A., Getmanets, V.F. and Ernigorenko, B.V. Thermal insulation of cryogenic pipelines with small diameters. Inz-Fiz-Zu, (1984) 47 64-71.

62 Ohmori, T. Thermal performance of evacuated multilayer insulation - Fabricated on the horiontally supported thermal shield (Private communication, 1992 - Paper in Japanese).

63 Glassford, A.P.M., Osiecki, R.A. and Liu, C.K. Effect of temperature and preconditioning on the outgassing rate of double aluminized mylar and dacron net. J. Vac. Sci. Technol (1984) A2 (3) 1370-1377.

64 Price, J.W. Measuring the gas pressure within a high performance insulation blanket. Adv. Cryog. Eng. (1967) 13 662-670.

65 Jacob, S., Kasthurirengan, S. and Karunanithi, R. Measurement of interlayer gas pressure in multilayer insulations. Proc. ICEC-12 (1988) 152-154.

66 Verkin, B.I., Mikhalchenko, R.S., Getmanetz, V.F. and Mikheev, V.A., Application of multilayer insulation in cryogenic engineering and improvement of its efficiency. Proc. ICEC-10 (1984) 529-538.

67 Price, J.W. and Lee, T.G. Analysis, Design and testing of heat-short-isolation components for high performance insulation systems. Adv. Cryog. Eng. (1966) 12 265-273.

68 Danielsson, H., Lebrun, P., and Rieubland, J.-M. Precision heat leak measurements on cryogenic components at 80 K, 4.2 K and 1.8 K, Cryogenics ICEC Supplement (1992) 32 215-217.

69 Ohmori, T., and Takahashi, K., Thermal performance of evacuated multilayer insulation, Proc. Thermal Engg. Symposium (ISME), (1992), No: 920-57, 48-49 (Private Communication on the above publication).

Fig. 17 (a) Experimental arrangement of the cylindrical calorimeter at IHI [11]

Fig. 17 (b) Modified experimental system at IHI [62]

Fig. 18 Test cryostat at DESY [45]

Fig. 19 Cylindrical calorimeter at Mitsubishi [21]

Fig. 20 Double guarded cylindrical calorimeter at IISc Bangalore [48]
1. FRP tube; 2. lower guard chamber; 3. Teflon spacer; 3. test chamber; 5. copper wool; 6. upper guard chamber; 7. pump-out port; 8. brass bush; 9. Penning gauge; 10. needle valve; 11. Pirani gauge; 12. thermocouples.

Fig. 21 Single guarded flat cold plate calorimeter at ADL [19]

Fig. 22 Double guarded flat cold plate calorimeter at ADL [10]

Fig. 23 Flat-plate device for measuring the thermal conductivity coefficient of insulating materials at different mechanical loads with the double controlling of the heat flux [23].
1--bell jar; 2--measuring vessel; 3--guard vessel; 4--shield vessel; 5--insulation investigated; 6--measuring heater; 7--guard heater; 8--system of mechanical loads.

Fig. 24 (a) Flat vertical cold plate calorimeter at Fermi Laboratory [9]
A, 4.2-K fin; B, rectangular 77-K box; C, inner helium vessel; D, outer helium vessel; E, nitrogen vessel; F, vent tube.

Fig. 24 (b) Flat vertical cold plate calorimeter (277 - 77 K) system at Fermi Laboratory [20]

Fig. 25 Flat hot plate calorimeter at the Institute for low temperature and structural research, Poland [51]
1, Vacuum port; 2, upper chamber; 3, outer shell; 4, lower chamber; 5, thermal screen; 6, modified heat-sink; 7, flange connection; 8, cold plate (with 100 Ω manganin heater); 9, mylar sceen; 10, guard plate (with 100 Ω manganin heater); 11, measuring plate (with 400 Ω manganin heater; the heater for the measuring heat flux emission); 12, tested sample; 13, guard ring, made of tested sample material; 14,

thermal screen, lower part; 15, outer shell, lower part; 16, thermal screen,. copper ring; 17, reference point of thermocouple (with platinum thermometer); 18, small Dewar container; 19, electrical feed-through; 20, necks)

Fig. 26 Flat hot plate calorimeter at Institute for Low Temperature Physics and Engineering, Kharkov [52]

Fig. 27 Flat vertical cold plate calorimeter at Mitsubishi laboratory [21]

Fig. 28 Tank calorimeter at Cryogenic Engineering Co. USA [7]

Fig. 29 Tank calorimeter at Lockheed Research Laboratories [54]

Fig. 30 Tank calorimeter at Institute for Low Temperature and Structural Research, Poland [18]

Fig. 31 Rectangular test tank at KfK [56]

Fig. 32 TESSI test bench at KfK [28]

Fig. 33 Modified heat leak facility at Fermi Laboratory for MLI measurements [39]

Table 1: Overall maximum error in the estimation of effective thermal conductivity (K_{eff})

Author + Reference	Type of Calorimeter	Warm and cold boundary temperatures	Maximum error ± %
Golovanov [23]	Flat plate [boil off + electrical input]	293 K - 77.6 K	8.4 - 33.4
Halaczek and Rafalowicz [18]	Flat hot plate	295 K - 87 K	8 - 10
Black et al. [19]	Single guarded Flat cold plate	277 K - 77 K	8
Black et al. [24]	Double guarded Flat cold plate	300 K - 20 K	9
Coston and Ziermann [17]	Double guarded Flat cold plate	300 K - 20 K	10
Leung et al. [9]	Vertical cold plate [Plate-in-Box]	300 K - 4.2 K	10
Coston and Ziermann [17]	Double guarded Cylindrial	300 K - 77 K	15
De Hann [7]	Tank calorimeter	300 K - 20 K	11
Halaczek and Rafalowicz [18]	Tank calorimeter	$\Delta T = 177$ K	20

Table 2: Performance Data of MLI from various Calorimeteric Investigations

No.	Calorimeter and Reference	Radiation shield	Thermal spacer	Insulation thickness	No. of Layers	Layer density	Cold boundary temp. (K)	Warm boundary temp. (K)	Heat flux W/m^2	Effective thermal conductivity $\mu W\ cm^{-1}\ K^{-1}$
1	Double guarded cylindrical [1] (Kropshot et al.)	Al. foil 0.0023 inch	Dexter glass paper 0.0048 inch	1.5 inch	75	50 layer per inch	76 20	300 300		0.52 0.42
2	Double guarded cylindrical [43] (Hnilicka)	NRC-2	---	1/2 inch	25		77	300	0.78	
3	Double guarded cylindrical [3] (Scurlock and Saull)	Al. foil 8.7 μm	Carbon loaded fiber glass paper	0.324 cm	10		77	300	0.517	0.077
4	Double guarded cylindrical [44] (Matsuda and Yoshikiyo)	Composite (a) polyester with aluminzed (b)Carbon loaded	insulation non-oven fabric one side(100nm) (50 % cellulose paper)		10 10	2.7 layer per mm - do -	77 77	300 300		1.8 1.4
5 (a)	Double guarded cylindrical [11] (Ohmori et al.)	Dimpled Al. nized on both and 379 Å) Single aluminized Mylar 659 Å - do - 283 Å	Mylar (alumi- sides 505 Å IHI Japan Polyester net - do -		40 40 40 40	4.02 p.mm - do - 2.86 p.mm 2.86 p.mm	78 4.2 78 78	293 78 293 293	0.31 0.052 0.48 0.85	
5 (b)	Double guarded cylindrical [69] (Ohmori et al.)	IHI-DI-DAM	---		40 40	2.75 p.mm 2.75p.mm	77 4.2	302 77	0.163 0.008	0.105 0.016

Table 2: Performance Data of MLI from various Calorimeteric Investigations

No.	Calorimeter and Reference	Radiation shield	Thermal spacer	Insulation thickness	No. of Layers	Layer density	Cold boundary temp. (K)	Warm boundary temp. (K)	Heat flux W/m^2	Effective thermal conductivity $\mu W\ cm^{-1}\ K^{-1}$
6	Single guarded calorimeter [45] (Burmeister et al.)	NRC (Both side 400 Å) --- Dimpled Al.	glass net 80 g/m^2 --- Mylar (IHI)		20 --- 20		78 --- 78	293 --- 293	0.45 ± 0.06 --- 0.85 ± 0.06	
7	Double guarded cylindrical calorimeter [21] (Amano et al.)	Double aluminized Mylar 6 µm	Nylon netting		50	40 per cm	78	300	≃ 1.0	
8	Double guarded cylindrical calorimeter [48] (Jacob et al.)	Double aluminized Mylar 12 µm thick 0.4 % perforation	Nylon netting 80 µm		48	25 per cm	78.5	294	1.01	0.888
9	Single guarded rectangular calorimeter [46, 47] (Gathright and Reeve)	3 M tape			--	--	77 4.2	300 77	6.20 0.0125	
10	Flat vertical cold plate/plate-in-Box calorimeter. [9] Leung et al. and [20] Shu et al.	NRC - 2 single Mylar --- 3 M ≠ 425 Al.	aluminized (300 Å) --- tape		30 --- ---		77 4.2 --- 77 4.2	277 77 --- 277 77	0.54 0.0126 --- 4.8 0.0124	
11	Flat hot plate [18] Rafalowicz and Halaczek	Al. foil --- Al. foil	glass paper --- glass paper + 30 % carbon		10 --- 10		90 --- 90	295 --- 295	2.91 --- 3.89	0.569 --- 0.760

Table 2: Performance Data of MLI from various Calorimeteric Investigations

No.	Calorimeter and Reference	Radiation shield	Thermal spacer	Insulation thickness	No. of Layers	Layer density	Cold boundary temp. (K)	Warm boundary temp. (K)	Heat flux W/m^2	Effective thermal conductivity $\mu W\ cm^{-1}\ K^{-1}$
12	Tank calorimeter [53] Ruccia and Hinckley	1/2 mil aluminized Mylar 375 Å	Silk netting 2 layer per shield		5		77	300	3.15	--
13	Tank calorimeter [54] Nast et al.	Double aluminized Mylar 6 µ	Silk netting 130 µm	2.44 cm	37		135	290	0.25	0.30
14	Tank calorimeter [55] Nast et al.	Double aluminized Mylar 6 µ	- do -		9	13 per cm	77 4.2	300 80	1.15 ≃ 0.02	0.486
15	Tank calorimeter Tessi [56] Barth and Lehmann	Double aluminized Mylar (Jehier) (Blankets)	Polyester tulle		36 24		80 80	295 295	0.56 0.73	0.30
16	Heat meter - Fermi [41] Gonczy et al.	Double aluminized Mylar 25 µ Dimpled double side (IHP) + 2 layers DAM blanket (3 + 3 layers)	Fiberglass mat 254 µm -------		11 (20 + 6) = 26	1.7 per mm 4.55 per mm	80 80	300 300	2.44 0.618	0.72 0.16

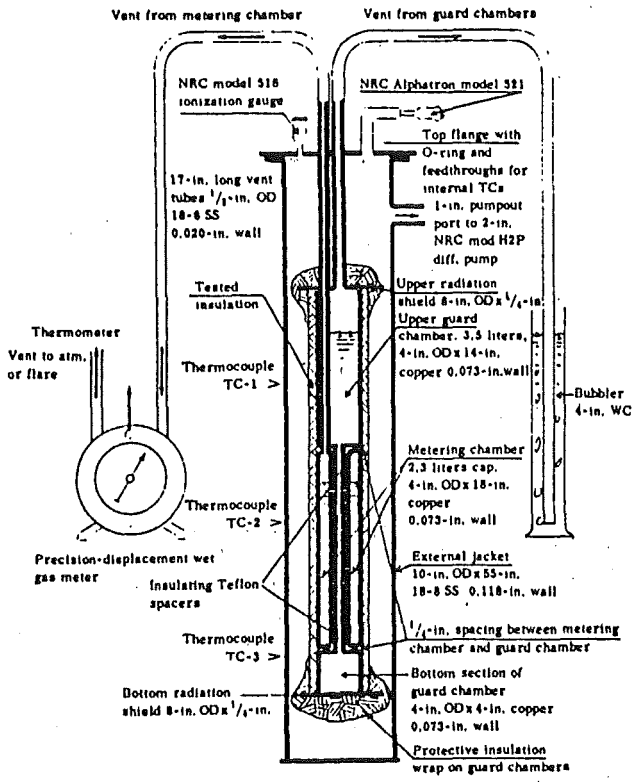

Fig. 1 NBS double guarded cylindrical calorimeter [1, 43]

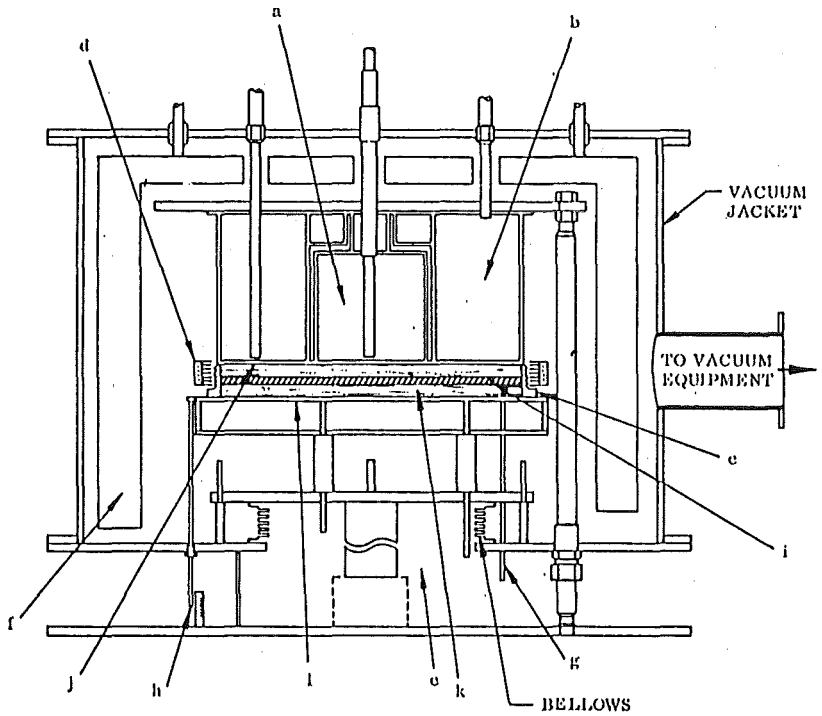

a. CALORIMETER RESERVOIR
b. GUARD RESERVOIR
c. ENCAPSULATING GAS BELLOWS
d. EDGE GUARD HEAT EXCHANGER
e. LOAD CHAMBER
f. OUTER RESERVOIR
g. INSTRUMENTATION PORTS
h. MICROMETER
i. WARM TEMPERATURE BOUNDARY HEATERS
j. INSULATION SPECIMEN
k. HEATER INSULATION
l. WATER COOLED SUPPORT RATE

Fig. 2 Flat plate calorimeter [17]

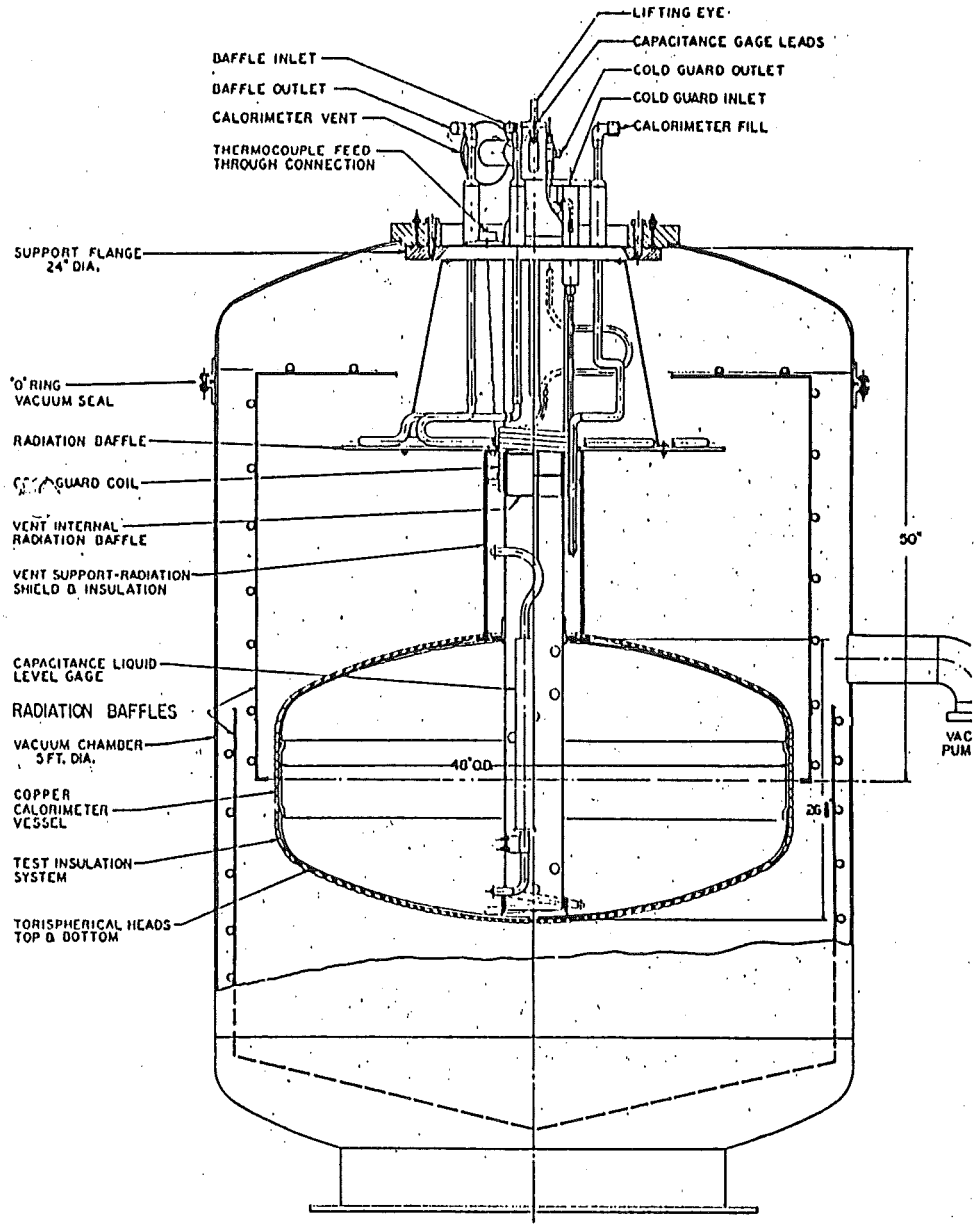

Fig. 3 Schematic of tank calorimeter [53]

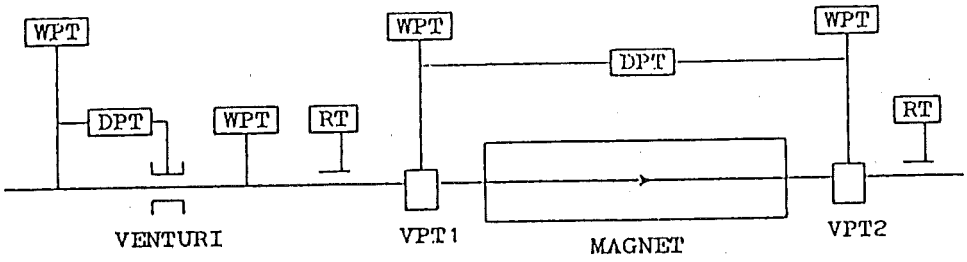

Fig. 4 Enthalpy difference method of heat leak estimation [29]
WPT - warm pressure transducer; DPT - differential pressure transducer;
VPT - vapour pressure thermometer; RT - resistance thermometer

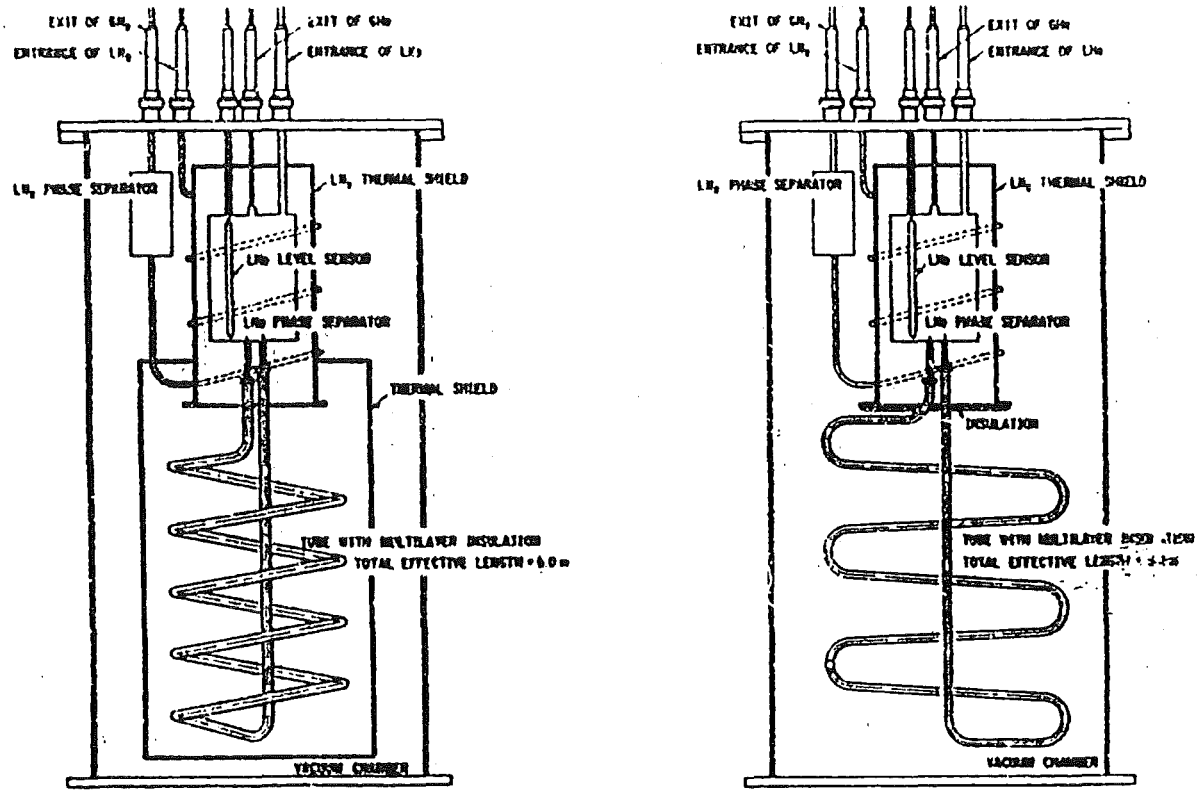

Fig. 5 Experimental arrangement to optimize insulation winding methods for cryogenic pipes [32]

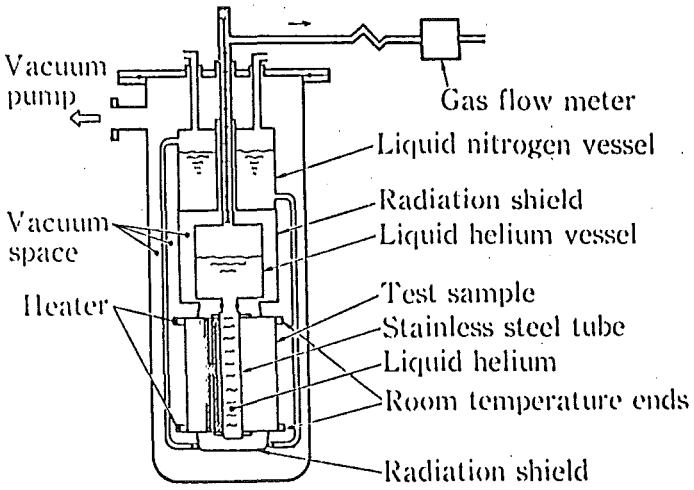

Fig. 6 Experimental apparatus to study heat leak to levitation magnet supports [23]

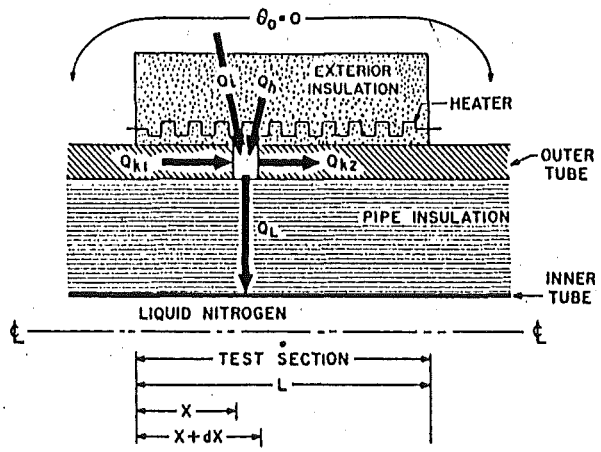

Fig. 7 Heat transfer to the outer wall in a test section of cryogenic pipe [34]

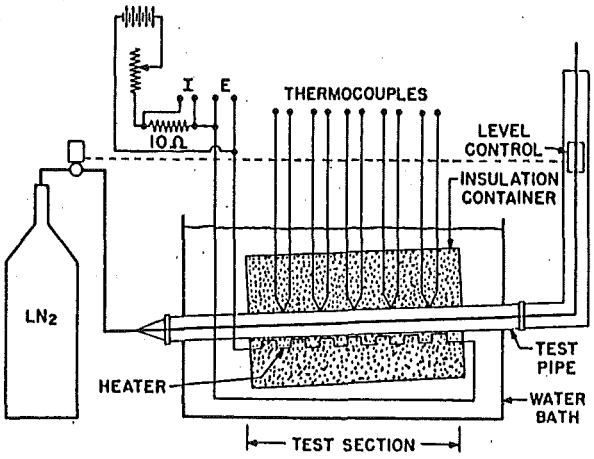

Fig. 8 Schematic of the apparatus for measuring the heat leak into a cryogenic pipe [34]

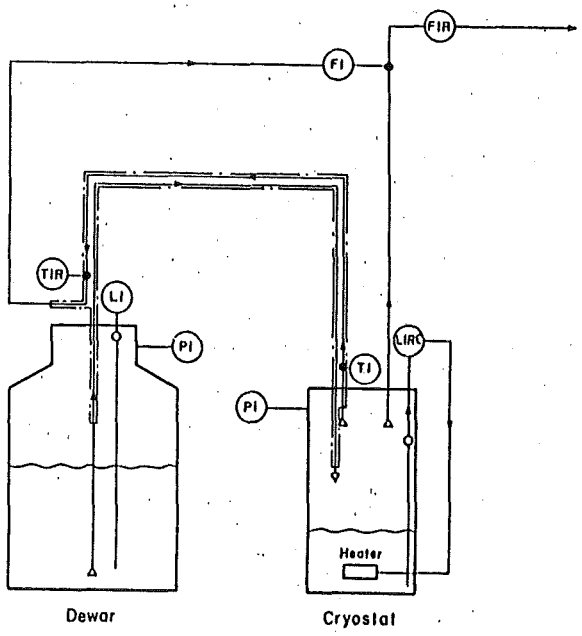

Fig. 9 Set-up for dynamic heat leak estimation of liquid helium transfer lines [35]

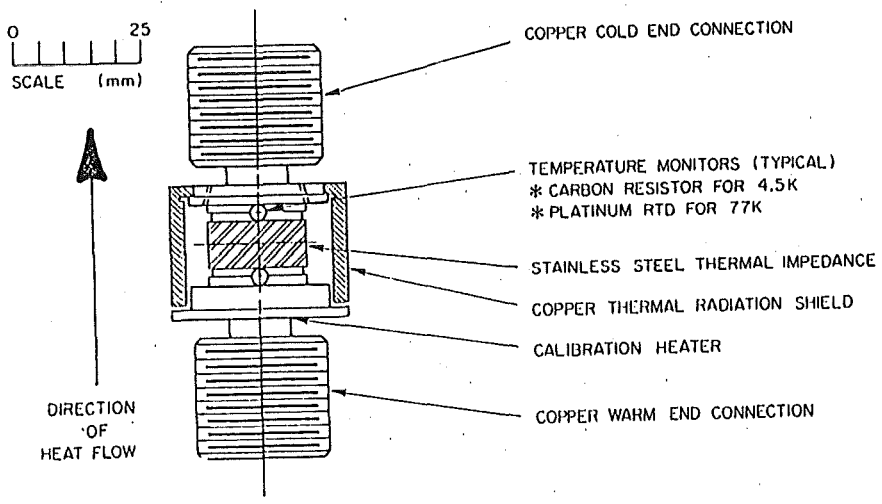

Fig. 10 Schematic of a heat meter [38]

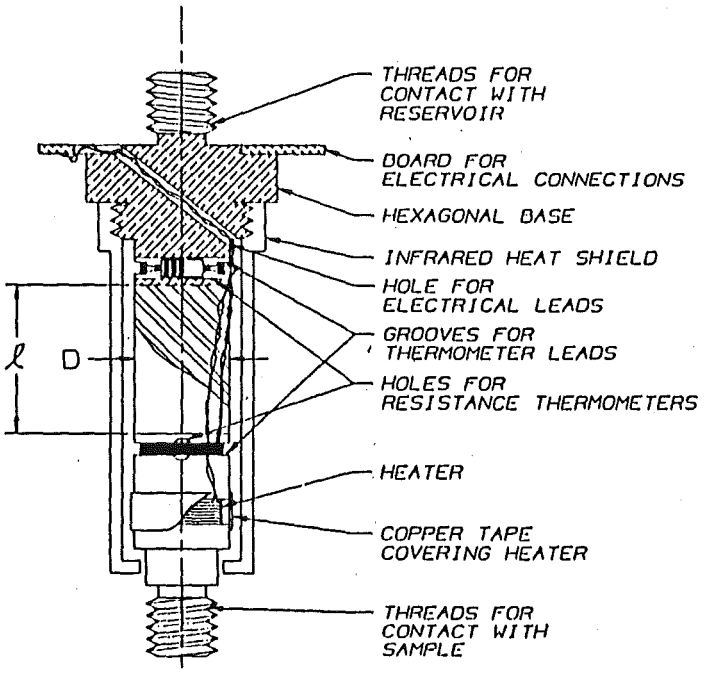

Fig. 11 Assembly drawing of a heat meter [37]

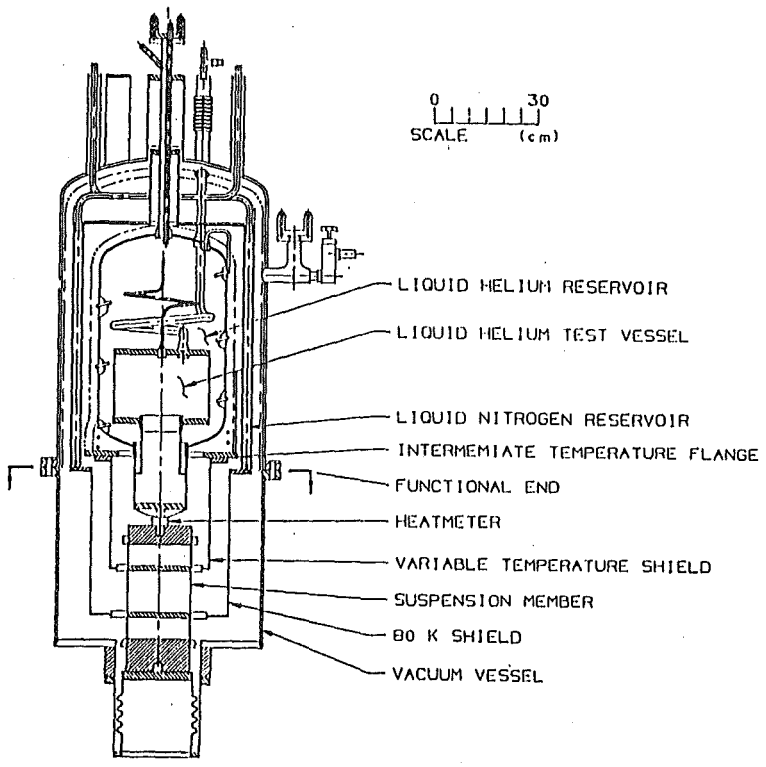

Fig. 12 Heat leak mesurement facility at Fermi laboratory [38]

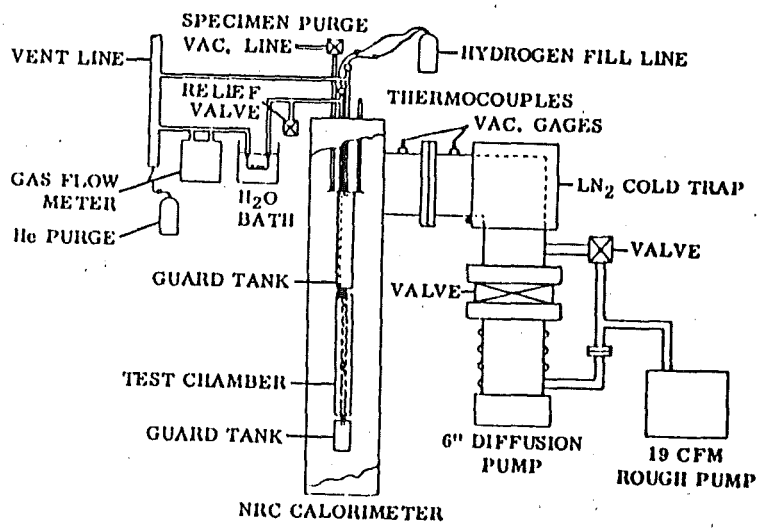

Fig. 13 Test calorimeter at General Dynamics, USA [27]

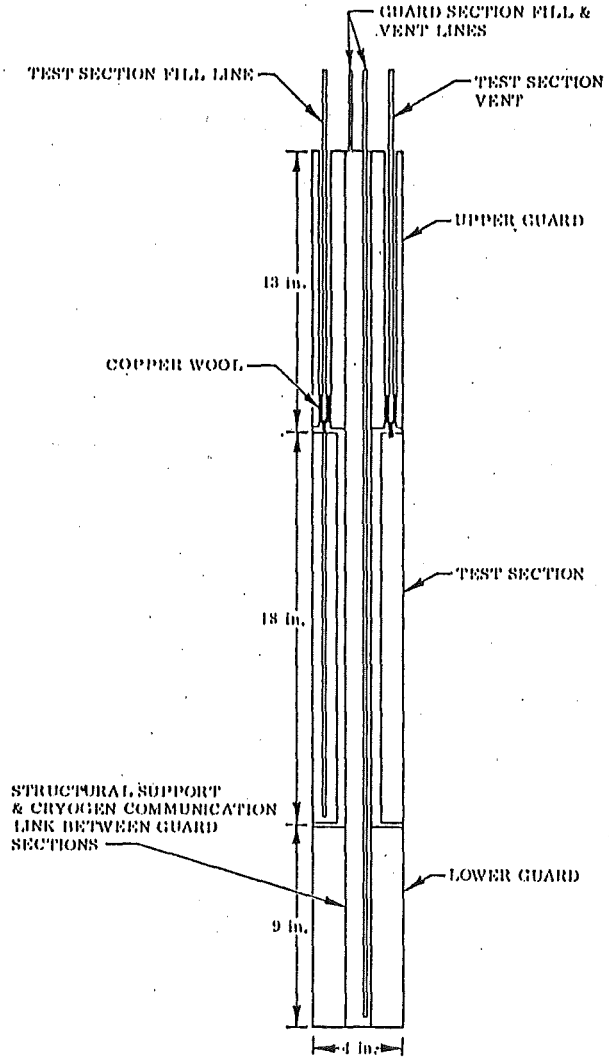

Fig. 14 Double guarded cylindrical calorimeter at Lockheed [17]

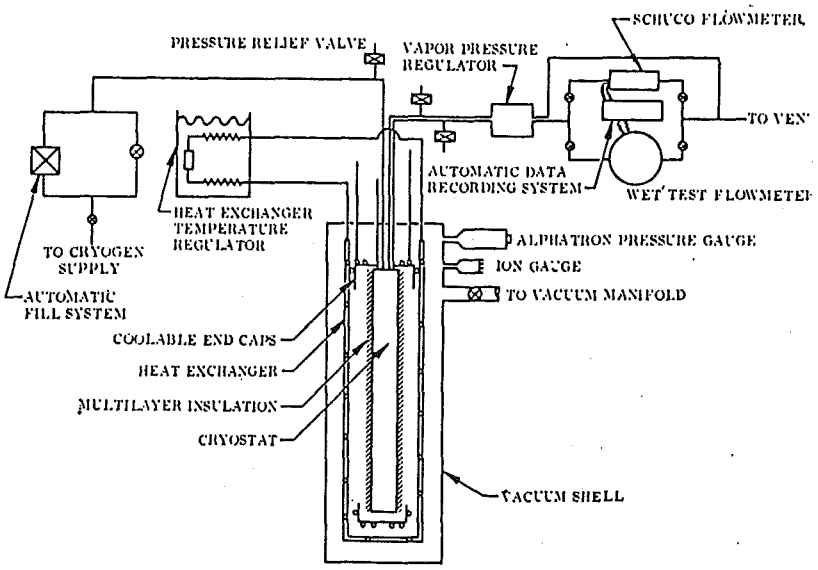

Fig. 15 Schematic of cryostat and associated instrumentation [17]

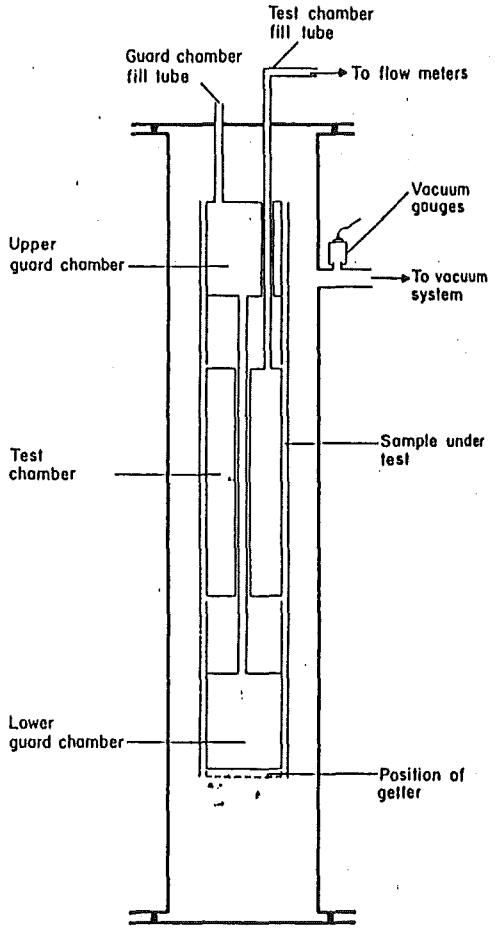

Fig. 16 Schematic of insulation test rig at Southampton University [3]

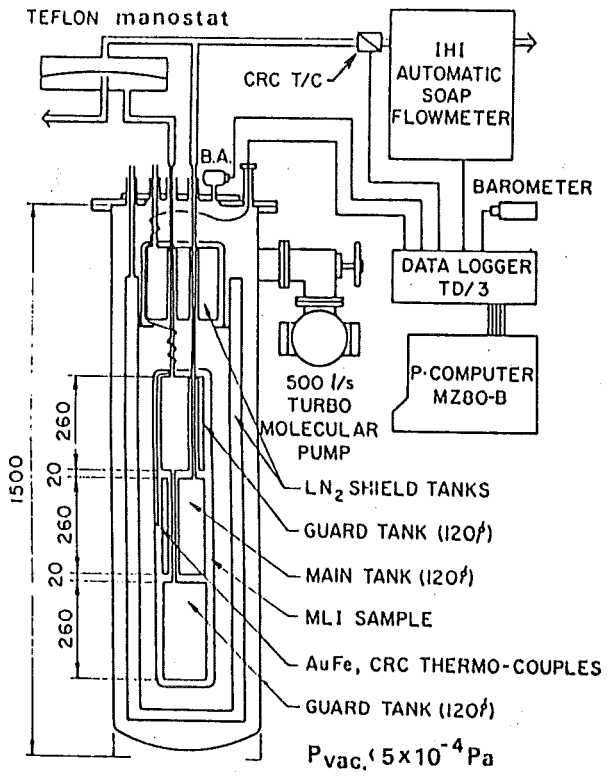

Fig. 17 (a) Experimental arrangement of the cylindrical calorimeter at IHI [11]

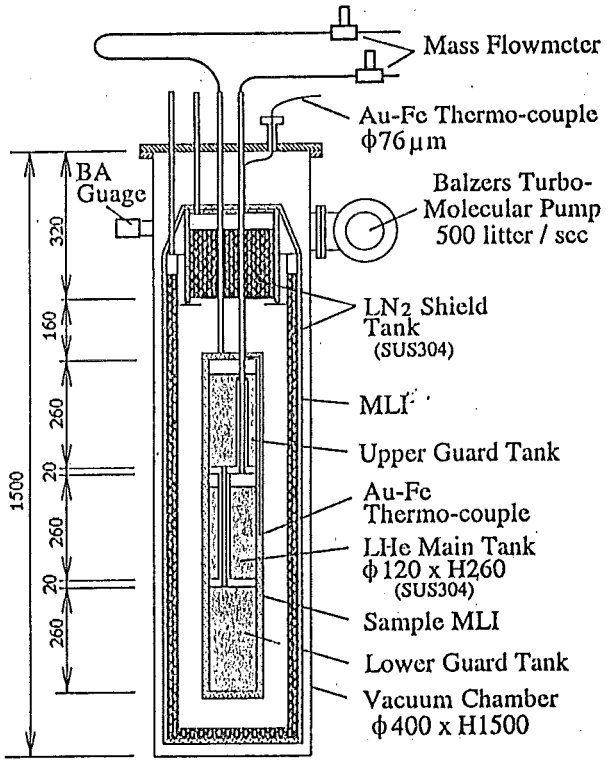

Fig. 17 (b) Modified experimental system at IHI [62]

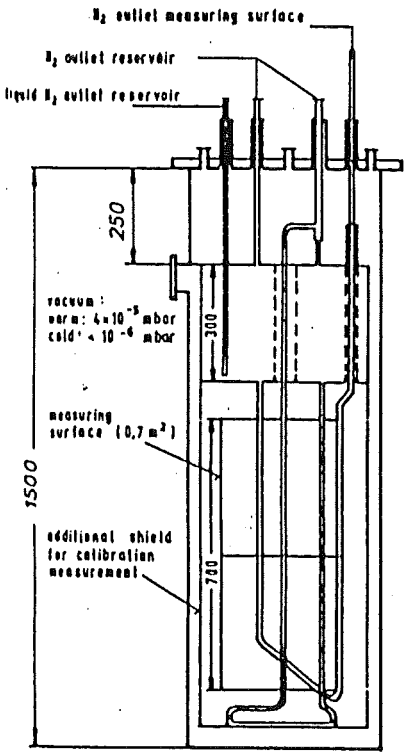

Fig. 18 Test cryostat at DESY [45]

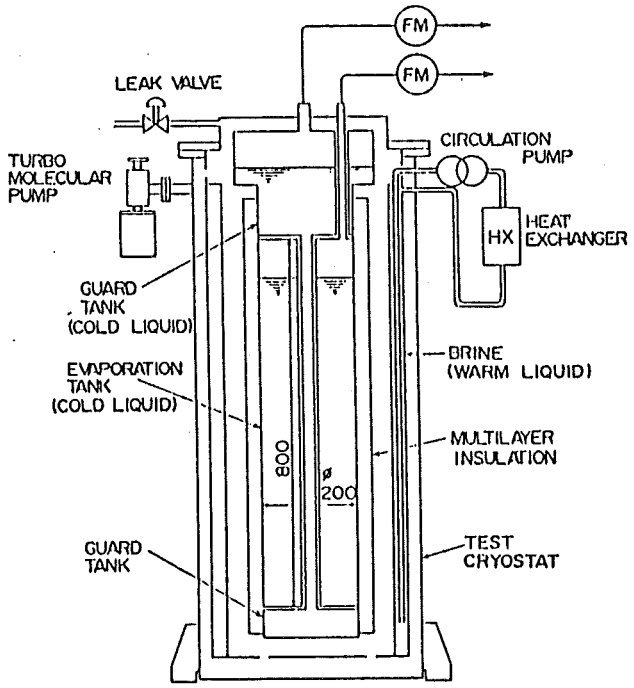

Fig. 19 Cylindrical calorimeter at Mitsubishi [21]

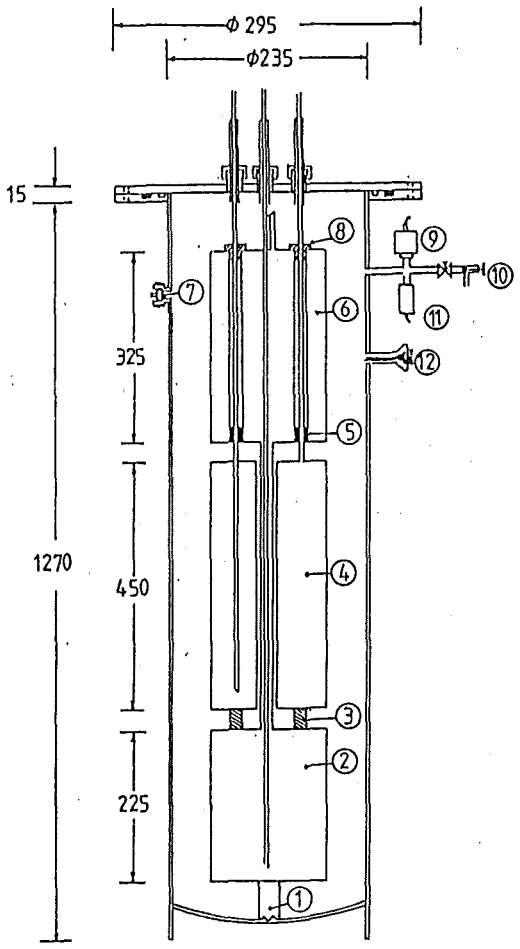

Fig. 20 Double guarded cylindrical calorimeter at IISc Bangalore [48]

1. FRP tube; 2. lower guard chamber; 3. Teflon spacer; 3. test chamber; 5. copper wool; 6. upper guard chamber; 7. pump-out port; 8. brass bush; 9. Penning gauge; 10. needle valve; 11. Pirani gauge; 12. thermocouples.

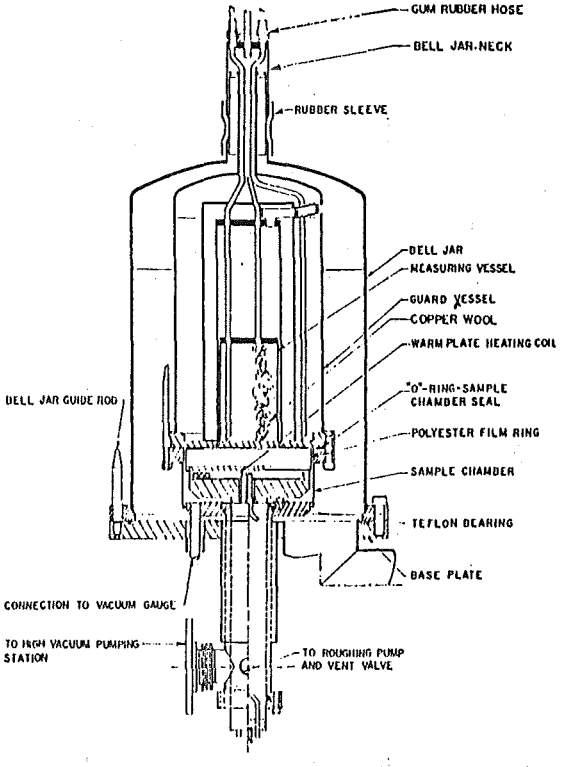

Fig. 21 Single guarded flat cold plate calorimeter at ADL [19]

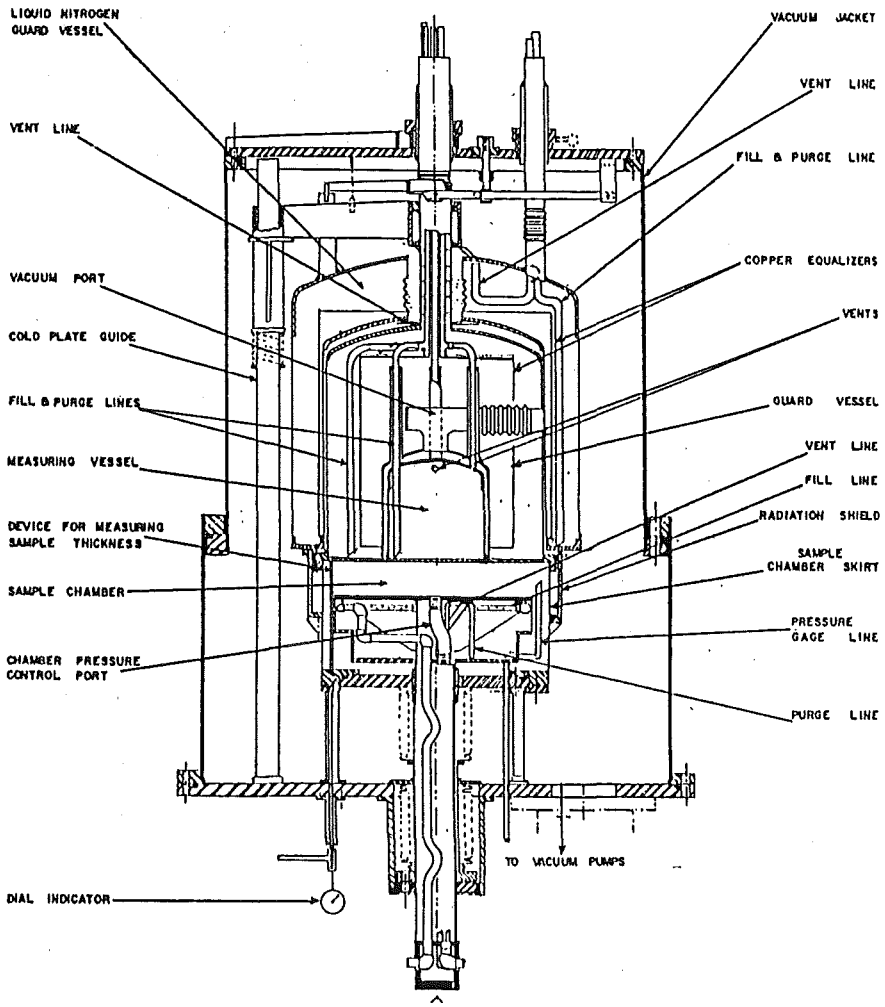

Fig. 22 Double guarded flat cold plate calorimeter at ADL [10]

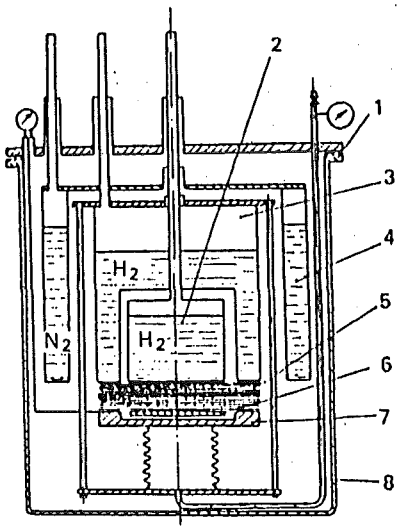

Fig. 23 Flat-plate device for measuring the thermal conductivity coefficient of insulating materials at different mechanical loads with the double controlling of the heat flux [23].

1--bell jar; 2--measuring vessel; 3--guard vessel; 4--shield vessel; 5--insulation investigated; 6--measuring heater; 7--guard heater; 8--system of mechanical loads.

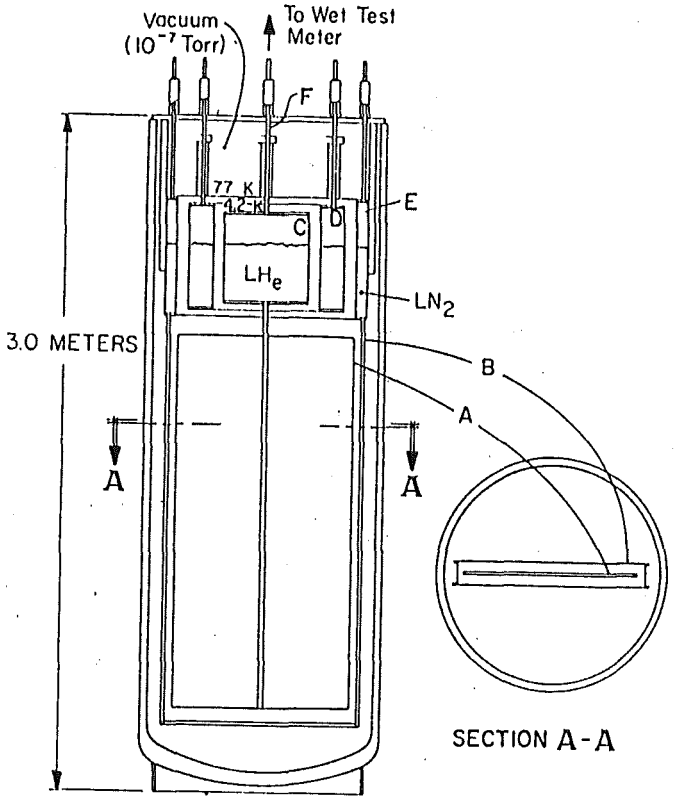

Fig. 24 (a) Flat vertical cold plate calorimeter at Fermi Laboratory [9]

A, 4.2-K fin; B, rectangular 77-K box; C, inner helium vessel; D, outer helium vessel; E, nitrogen vessel; F, vent tube.

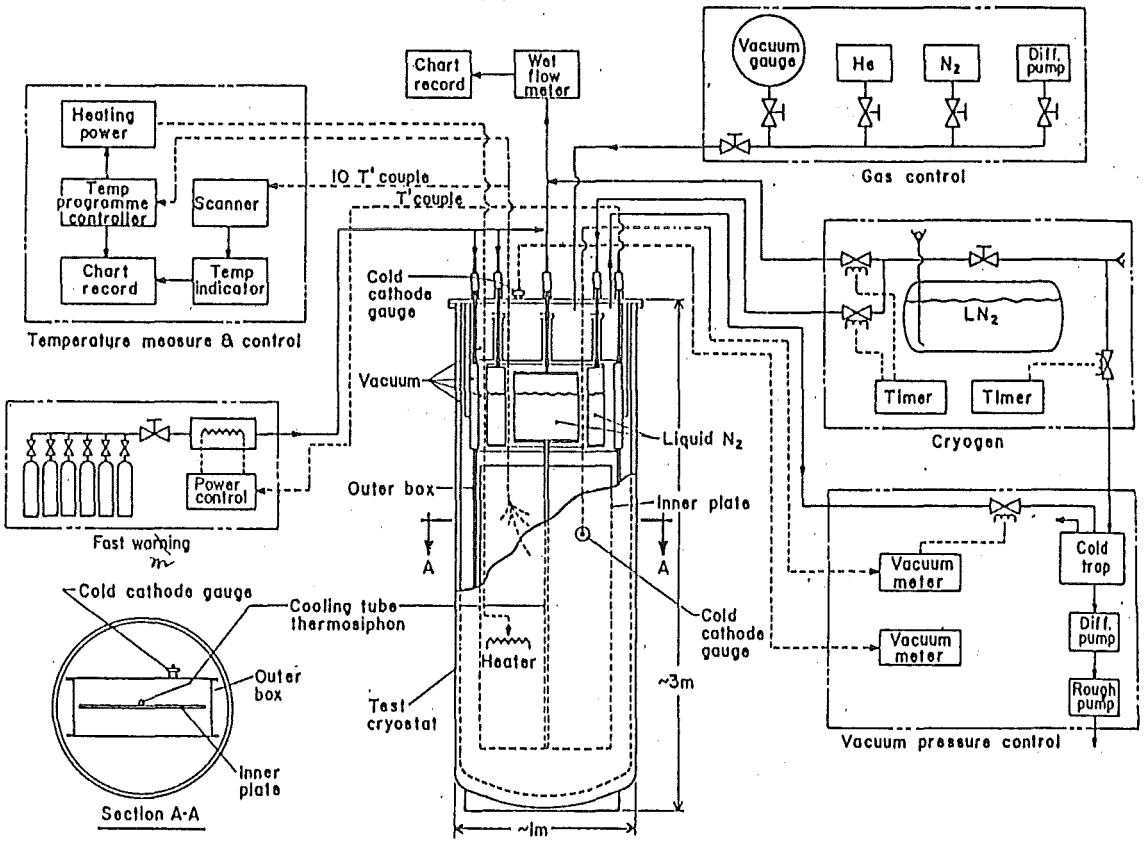

Fig. 24 (b) Flat vertical cold plate calorimeter (277 - 77 K) system at Fermi Laboratory [20]

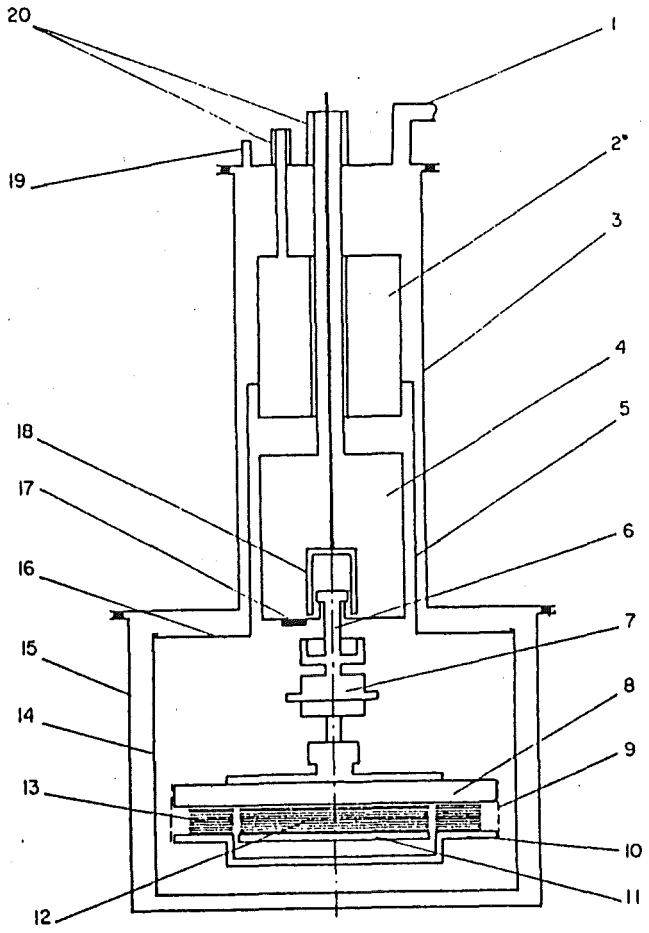

Fig. 25 Flat hot plate calorimeter at the Institute for low temperature and structural research, Poland [51]

1, Vacuum port; 2, upper chamber; 3, outer shell; 4, lower chamber; 5, thermal screen; 6, modified heat-sink; 7, flange connection; 8, cold plate (with 100 Ω manganin heater); 9, mylar sceen; 10, guard plate (with 100 Ω manganin heater); 11, measuring plate (with 400 Ω manganin heater; the heater for the measuring heat flux emission); 12, tested sample; 13, guard ring, made of tested sample material; 14, thermal screen, lower part; 15, outer shell, lower part; 16, thermal screen,. copper ring; 17, reference point of thermocouple (with platinum thermometer); 18, small Dewar container; 19, electrical feed-through; 20, necks)

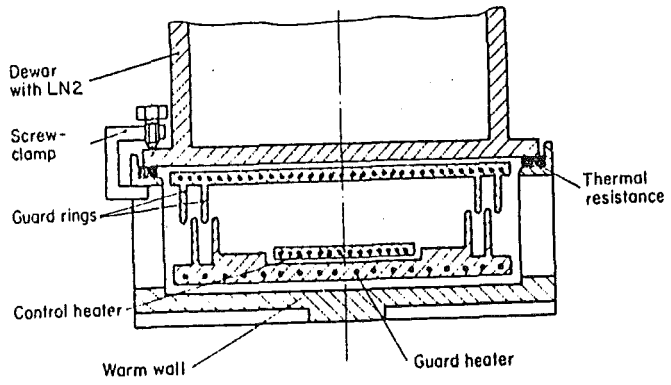

Fig. 26 Flat hot plate calorimeter at Institute for Low Temperature Physics and Engineering, Kharkov [52]

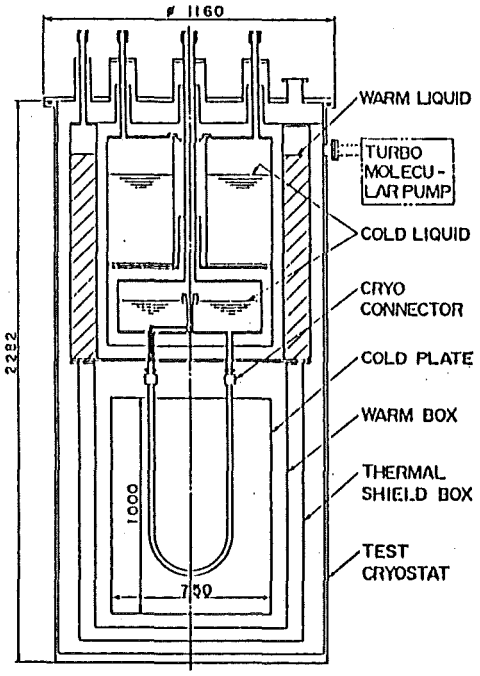

Fig. 27 Flat vertical cold plate calorimeter at Mitsubishi laboratory [21]

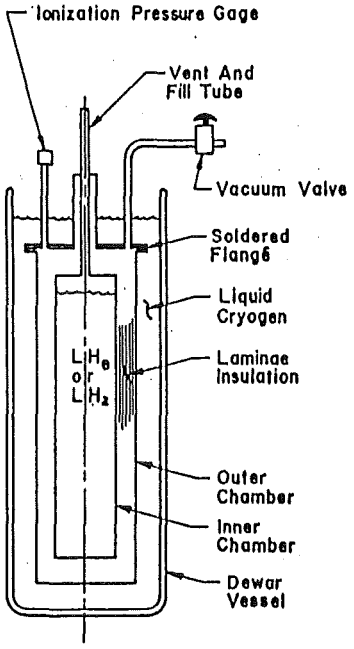

Fig. 28 Tank calorimeter at Cryogenic Engineering Co. USA [7]

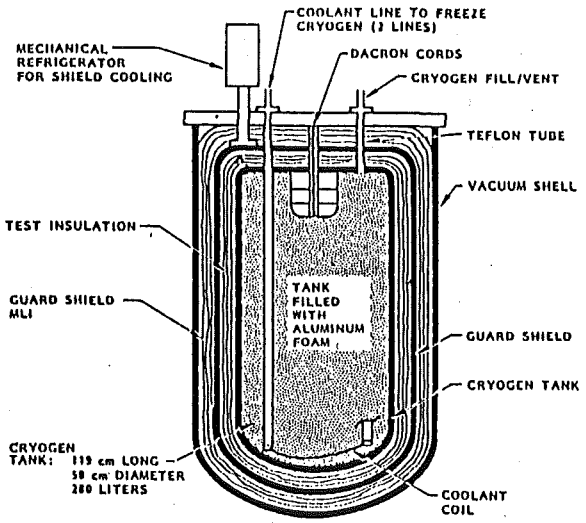

Fig. 29 Tank calorimeter at Lockheed Research Laboratories [54]

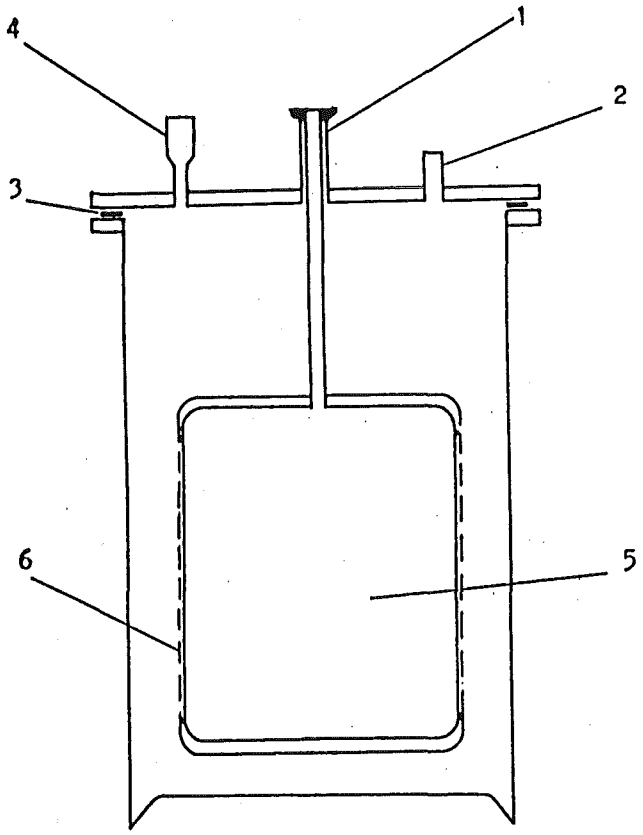

Fig. 30 Tank calorimeter at Institute for Low Temperature and Structural Research, Poland [18]

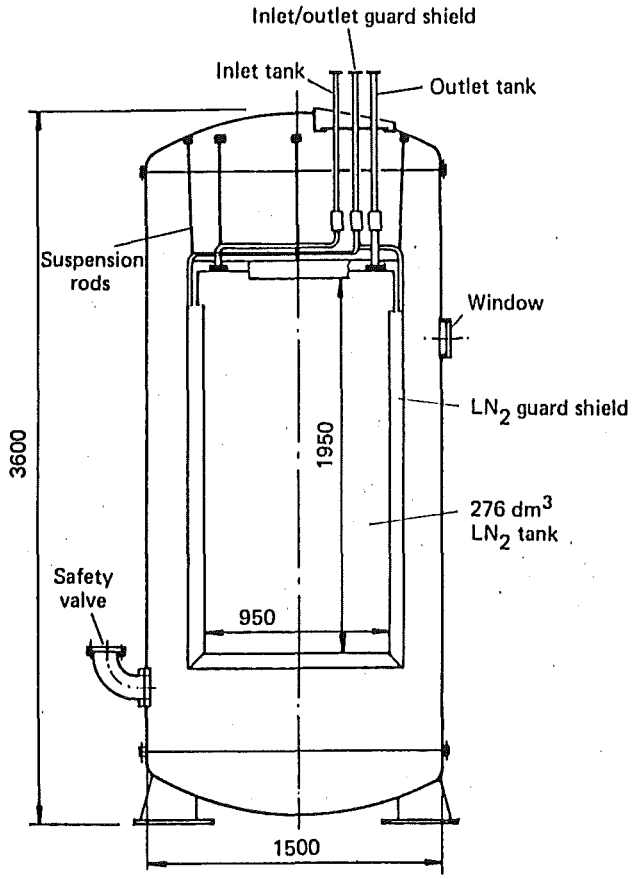

Fig. 31 Rectangular test tank at KfK [56]

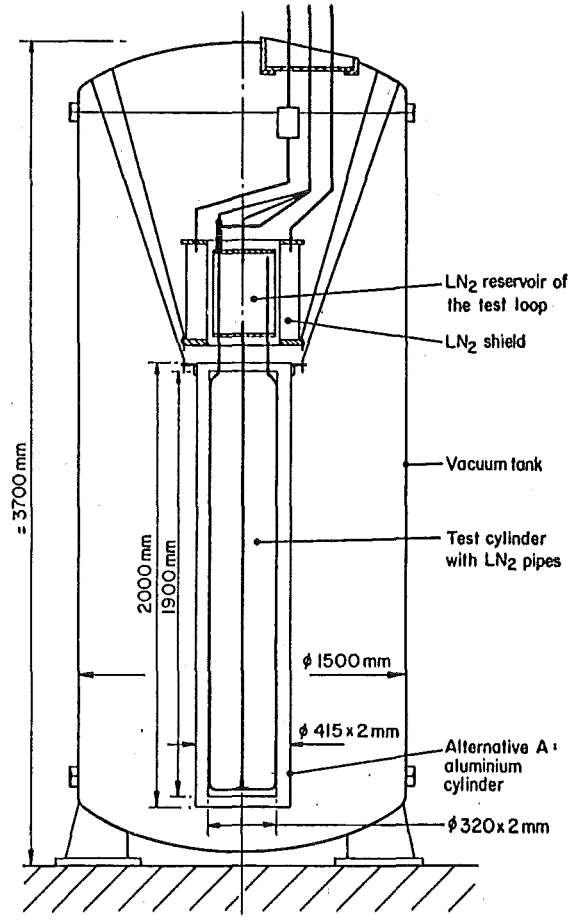

Fig. 32 TESSI test bench at KfK [28]

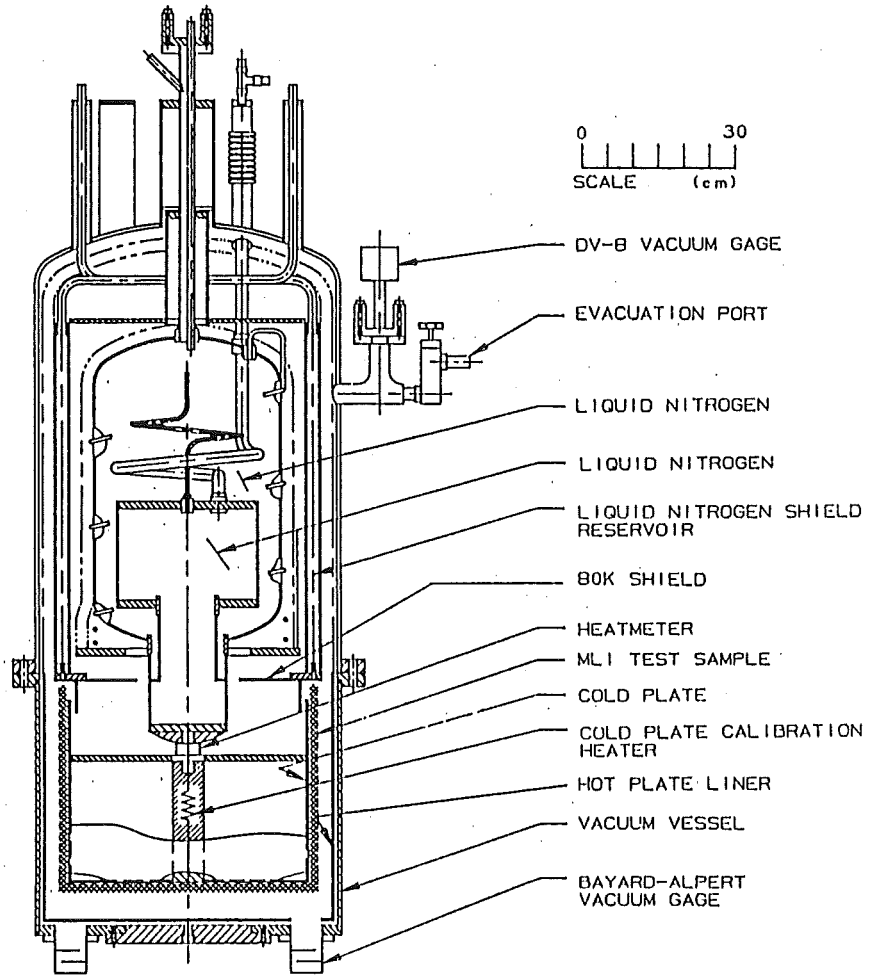

Fig. 33 Modified heat leak facility at Fermi Laboratory for MLI measurements [39]